



**T.C.
ISTANBUL UNIVERSITY-CERRAHPASA
INSTITUTE OF GRADUATE STUDIES**



M.Sc. THESIS

**PREPARATION OF THE MESOPOROUS SCAFFOLDS FOR DRUG
DELIVERY AND RELEASE SYSTEMS**

MONA H. ALI BNHMAD

SUPERVISOR

Prof. Dr. Ayşe Zehra AROĞUZ

Department of Chemistry

Chemistry Programme

ISTANBUL-

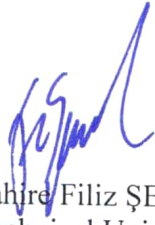
March, 2019

This study was accepted on 20/3/2019 as a M. Sc. thesis in Department of Chemistry, Chemistry Programme by the following Committee.

Examining Committee Members



Prof. Dr. Ayşe Zehra AROĞUZ(Supervisor)
İstanbul University-Cerrahpaşa
Faculty of Engineering



Prof. Dr. Bahire Filiz ŞENKAL
İstanbul Technical University
Science and Letters Faculty



Prof. Dr. Sema DEMİRCİ ÇEKİC
İstanbul University-Cerrahpaşa
Faculty of Engineering



As required by the 9/2 and 22/2 articles of the Graduate Education Regulation which was published in the Official Gazette on 20.04.2016, this graduate thesis is reported as in accordance with criteria determined by the Institute of Graduate Studies by using the plagiarism software to which Istanbul University-Cerrahpasa is a subscriber.

FOREWORD

I give praise to **Allah Almighty**, who gave me the strength to pursue this research study and complete it by granting me the opportunity and the ability to proceed till the end.

All of my appreciation and thanks to my supervisor **Prof. Dr. Ayşe Zehra AROĞUZ**, for her continuous effective guidance, patience, and support during the research study and writing of my thesis.

I would like to thank **Halis Can Mörel** for his support in this work.

I also thank to **Ass. Prof. Dr. Davut Lacin** for the XRD analysis and his valuable comments.

I also extend my thanks to my country which offered me the financial resources to pursue M.SC. Degree study.

All thankfulness to my husband **Salah Elkaylani**, who supported me with love and understanding throughout.

Last but not least, I wish to dedicate my special thanks to **my beloved parents** for their ceaseless encouragement and their support, and also, my brothers, sisters, my daughters, and friends who supported me throughout this thesis and believed in me, this achievement wouldn't be done without all of them.

March 2019

MONA H. ALI BNHMAD

TABLE OF CONTENTS

	Page
FOREWORD	iv
TABLE OF CONTENTS	v
LIST OF FIGURES	viii
LIST OF TABLES	xi
LIST OF SYMBOLS AND ABBREVIATIONS	xii
ÖZET	xiii
SUMMARY	xiv
1. INTRODUCTION	1
1.1. THE MESOPOROUS MATERIALS	3
1.1.1. What are nanoparticles (NPs)?	3
1.1.2. Characterization techniques of NPs.....	6
1.1.3. Where are nanoparticles used?	7
1.1.4. Macroporous, mesoporous, microporous materials.....	7
1.1.5. Definition of mesoporous materials	9
1.1.6. Synthesis of mesoporous materials	9
1.1.6.1. <i>Bottom-up synthesis</i>	10
1.1.6.2. <i>Top-down synthesis</i>	10
1.1.7. Mesoporous silicate materials	10
1.2. DRUG DELIVERY SYSTEM	12
1.2.1. Definition of drugs	12
1.2.2. What is “a drug delivery system”?	12
1.2.3. Need for controlled delivery system.....	13
1.2.4. Mesoporous materials for drug loading and drug delivery system	13
1.3. WHAT IS DRUG RELEASE?	15
1.3.1. The drug delivery systems commonly used polymers	16
1.4. RELEASE KINETIC THEORIES.....	17
1.4.1. Zero order	17
1.4.2. First order	17
1.4.3. Higuchi model	18
1.4.4. Peppas model.....	18

2. MATERIALS AND METHODS	19
2.1. MATERIALS	19
2.2. INSTRUMENTS:	24
2.2.1. UV-VIS spectrophotometer	24
2.2.2. FT-IR instrument	24
2.2.3. SEM instrument	25
2.2.4. Sputter coater	25
2.2.5. XRD Instrument	26
2.2.6. BET Analysis	26
2.3. METHODS	27
2.3.1. Synthesize of mesoporous silica nanoparticles (MSNs)	27
2.3.2. Loading of 5-Fluorouracil and ciprofloxacin drugs	28
2.3.3. Drug release efficiency measurements	29
3. RESULTS	30
3.1. FT-IR STUDIES	30
3.1.1. FT-IR spectrum of TEOS	30
3.1.2. FT-IR spectra of 5-Fluorouracil and Ciprofloxacin drugs	30
3.1.3. FT-IR spectra of BMM before and after calcination	31
3.1.4. FT-IR spectra of BMM with drugs loaded	32
3.1.5. FT-IR spectra of TWN60 before and after calcination	33
3.1.6. FT-IR spectra of TWN60 with drugs loaded	34
3.1.7. FT-IR spectrum of TWN80 before and after calcination	35
3.1.8. FT-IR spectra of TWN80 with drugs loaded	36
3.2. SEM STUDIES:	37
3.2.1. SEM micrograph of BMM	38
3.2.2. SEM micrograph of TWN 60	39
3.2.3. SEM micrograph of TWN 80	41
3.3. XRD AND BET STUDIES:	44
3.3.1. XRD studies of BMM, TWN60, TWN80	44
3.3.2. BET studies:	45
3.4. WEIGHT LOSS CALCULATION OF THE SAMPLES	45
3.5. DRUG RELEASE AND DELIVERY STUDIES	46
3.5.1. Standard Curve of 5-Fluorouracil	46
3.5.2. Delivery and release of 5-Fluorouracil loaded to BMM	47

3.5.3.	Delivery and release of 5-Fluorouracil loaded to TWN60	48
3.5.4.	Delivery and release of 5-Fluorouracil loaded to TWN80	49
3.5.5.	Standard Curve of Ciprofloxacin.....	50
3.5.6.	Delivery and release of Ciprofloxacin loaded to BMM	51
3.5.7.	Delivery and release of Ciprofloxacin loaded to TWN60	52
3.5.8.	Delivery and release of Ciprofloxacin Loaded to TWN 80	53
4.	DISCUSSION	54
5.	CONCLUSION AND RECOMMENDATIONS.....	60
	REFERENCES	61
	CURRICULUM VITAE	68



LIST OF FIGURES

	Page
Figure 1.1: Various types of nanostructures [27].	6
Figure 1.2: The porous materials and its diameter.	8
Figure 1.3: Nanoparticles different methods of synthetic.	9
Figure 1.4: Nanoparticles of mesoporous silica image using (TEM).	11
Figure 1.5: Silica mesoporous materials and their use in drug delivery systems.	15
Figure 2.1: Chemical structure of cetyl-trimethylammonium bromide.	19
Figure 2.2: Chemical structure of Tetraethyl orthosilicate (TEOS).	20
Figure 2.3: Chemical structure of Fluorouracil molecule.	20
Figure 2.4: Chemical structure of Ciprofloxacin.	21
Figure 2.5: Chemical structure of (TritonX-100).	21
Figure 2.6: Chemical structure of TWEEN60.	22
Figure 2.7: Chemical structure of TWEEN 80.	23
Figure 2.8: UV-VIS spectrophotometer.	24
Figure 2.9: FT-IR Instrument.	25
Figure 2.10: SEM instrument.	25
Figure 2.11: sputter coater.	26
Figure 2.12: XRD Instrument.	26
Figure 2.13: BMM synthesized schematically.	27
Figure 2.14: Synthesis steps of silica mesoporous.	28
Figure 3.1: FTIR spectrum of TEOS.	30
Figure 3.2: FTIR spectrum of 5-Fluorouracil.	31
Figure 3.3: FTIR spectrum of Ciprofloxacin.	31
Figure 3.4: FTIR spectrum of BMM before calcination.	32

Figure 3.5: FTIR spectrum of BMM after calcination.	32
Figure 3.6: FTIR spectrum of BMM loaded with 5-Fluorouracil.	33
Figure 3.7: FTIR spectrum of BMM loaded with Ciprofloxacin.	33
Figure 3.8: FTIR spectrum of TWN60 before calcination.	34
Figure 3.9: FTIR spectrum of TWN60 after calcination.	34
Figure 3.10: FTIR spectrum of TWN60 loaded with 5-Fluorouracil.	35
Figure 3.11: FTIR spectrum of TWN60 loaded with Ciprofloxacin.	35
Figure 3.12: FTIR spectrum of TWN80 before calcination.	36
Figure 3.13: FTIR spectrum of TWN80 after calcination.	36
Figure 3.14: FTIR spectrum of TWN80 loaded with 5-Fluorouracil.	37
Figure 3.15: FTIR spectrum of TWN80 loaded with Ciprofloxacin.	37
Figure 3.16: SEM micrograph of BMM before calcination.	38
Figure 3.17: SEM micrograph of BMM after calcination.	38
Figure 3.18: SEM micrograph of BMM with 5-Fluorouracil.	39
Figure 3.19: SEM micrograph of BMM with ciprofloxacin.	39
Figure 3.20: SEM micrograph of TWN 60 before calcination.	40
Figure 3.21: SEM micrograph of TWN 60 after calcination.	40
Figure 3.22: SEM micrograph of TWN 60 with 5-Fluorouracil.	41
Figure 3.23: SEM micrograph of TWN60 with Ciprofloxacin.	41
Figure 3.24: SEM micrograph of TWN80 before calcination.	42
Figure 3.25: SEM micrograph of TWN80 after calcination.	42
Figure 3.26: SEM micrograph of TWN 80 with 5-Fluorouracil.	43
Figure 3.27: SEM micrograph of TWN80 with Ciprofloxacin.	43
Figure 3.28: XRD-patterns of BMM, TWN60, TWN80 (a) before calcination (b) after calcination.	45
Figure 3.29: Standard Curve of 5-Fluorouracil.	47
Figure 3.30: Release of 5-Fluorouracil loaded to BMM.	47

Figure 3.31: Release of 5-Fluorouracil loaded to TWN 60.....	48
Figure 3.32: Release of 5-Fluorouracil loaded to TWN 80.....	49
Figure 3.33: Standard Curve of Ciprofloxacin.....	50
Figure 3.34: Release of Ciprofloxacin Loaded to BMM.....	51
Figure 3.35: Release of Ciprofloxacin loaded to TWN 60.....	52
Figure 3.36: Release of Ciprofloxacin loaded to TWN 80.....	53



LIST OF TABLES

	Page
Table 1.1: Liposomes and Nanoparticles properties summary.....	4
Table 3.1: BET data of prepared samples after calcination precess.....	45
Table 3.2: Release constants of 5-Fluorouracil loaded to BMM in different media...	48
Table 3.3: Release constants of 5-Fluorouracil loaded to TWN 60 in different media.....	49
Table 3.4: Release constants of 5-Fluorouracil loaded to TWN 80 in different media.....	50
Table 3.5: Release constants of Ciprofloxacin Loaded to BMM in different media...	51
Table 3.6: Release constants of Ciprofloxacin Loaded to TWN 60 in different media.....	52
Table 3.7: Release constants of Ciprofloxacin loaded to TWN 80 in different media.....	53

LIST OF SYMBOLS AND ABBREVIATIONS

Abbreviation	Explanation
NPs	: Nanoparticles.
MSNs	: Mesoporous silica nanoparticles.
DDS	: Controlled drug delivery systems.
CTAB	: Cetyl-trimethylammonium bromide.
TEOS	: Tetraethyl orthosilicate.
TritonX-100	: Polyethyleneglycolp-(1,1,3,3-tetra methyl butyl)-phenyl ether.
TWN 60	: Resulted sample from the experiment which contain Tween60.
TWN 80	: Resulted sample from the experiment which contain Tween80.
BMM	: Resulted sample from the experiment (bi-model mesoporous).
TWN60_b, TWN60_w, TWN60_a	: The release of TWN60 in basic, aqueous, and acidic medium.
TWN80_b, TWN80_w, TWN80_a	: The release of TWN80 in basic, aqueous, and acidic medium.
BMM_w, BMM_b, BMM_a	: The release of BMM in basic, aqueous, and acidic medium.

ÖZET

YÜKSEK LİSANS TEZİ

İLAÇ YÜKLEME VE SALIM SİSTEMLERİ İÇİN MEZOGÖZENEKLI TUTUCULARIN HAZIRLANMASI

MONA H. ALI BNHMAD

İstanbul Üniversitesi-Cerrahpasa

Lisansüstü Eğitim Enstitüsü

Kimya Anabilim Dalı

Danışman : Prof. Dr. Ayşe Zehra AROĞUZ

Nanopartiküller (NPs) etkin ilaç taşıyıcılar olarak, ilaç yükleme ve salım sistemlerinde önemli bir rol oynamaktadırlar. Özellikle mezogözenekli nanopartiküllerin ilaç endüstrisinde kullanımı üzerinde yapılan bilimsel çalışmalar son yıllarda büyük hız kazanmıştır. İlaç salım proseslerinde, ilaç aktif maddenin belirli bölgeye veya ortama dağıtımının sağlanması istenilen bir durumdur. Mezogözenekli nanopartiküllerin ilaç yükleme ve salım sistemi olarak kullanılması ilaç endüstrisinde büyük bir gelişme olarak kabul edilmiştir. Bu çalışmanın amacı, üç ayrı mezogözenekli ilaç taşıyıcılar üzerinde iki farklı ilaç aktif maddesinin yükleme ve salımını incelemektir. Bu amaçla, BMM, TWN60 ve TWN80 olmak üzere üç çeşit mesoporous nanopartikül ilaç taşıyıcılar hazırlanmıştır. İlaç taşıyıcı olarak kullanılan bu iskele malzemelerin öncelikle yapısal ve morfolojik karakterizasyonları FTIR, SEM ve XRD cihazları ile incelenmiştir. Bu çalışmada hazırlanan tutucular üzerine model ilaç olarak seçilen 5-Fluorourasil ve Siprofloksasin İlaç aktif maddelerinin yüklemesi yapılmıştır. Yüklenen ilaçların salım kinetiği sıfırinci derece ve birinci derece kinetik denklemler ile Higuchi, Korsmeyer-Peppas kinetik modelleri kullanılarak incelenmiştir. Hazırlanan polimerik ilaç taşıyıcıların her iki ilaç aktif maddesi için etkin olarak kullanılabilirliği ortaya konulmuştur.

Mart 2019, 82 sayfa.

Anahtar kelimeler: Mezapor, nanopartikül, ilaç yükleme, ilaç salım, BMM, TWEEN60, TWEEN80, 5-florourasil, siprofloksasin.

SUMMARY

M.Sc. THESIS

PREPARATION OF THE MESOPOROUS SCAFFOLDS FOR DRUG DELIVERY AND RELEASE SYSTEMS

MONA H. ALI BNHMAD

Istanbul University-Cerrahpasa

Institute of Graduate Studies

Department of Chemistry

Supervisor : Prof. Dr. Ayşe Zehra AROĞUZ

Nanoparticles (NPs) are effective drug carriers as a result of their important roles in drug delivery and release systems. Recently, using of mesoporous nanoparticles have gained a great speed in scientific studies within the pharmaceutical industry. In the process of drug release, it is desirable to ensure releasing the drug active substance to a specific region or medium. The use of mesoporous nanoparticles as drug delivery and release systems are considered to be a major development within the pharmaceutical industry. The aim of this study is to investigate the loading and release profiles of two different drug active substances on three different mesoporous drug carriers. For this purpose, three mesoporous drugs carriers' nanoparticles: BMM, TWN60, TWN80 were prepared. The Structural and morphological characterizations of these scaffolds, used as drug carriers, were investigated via FTIR, SEM and XRD instruments. Model drug active substances 5-Fluorouracil and Ciprofloxacin were loaded onto these scaffolds. The kinetics release of the loaded drugs was investigated using zero and first order kinetic equations, Korsmeyer-Peppas and Higuchi kinetic models. It was found that the prepared polymer drug carriers can be effectively used to carry both of the drug active materials.

March 2019, 82 pages.

Keywords: Mesoporous, nanoparticles, drug delivery system, drug release system, BMM, TWEEN60, TWEEN80, 5- Fluorouracil, Ciprofloxacin

1. INTRODUCTION

Drug release systems had a remarkable development in the last few years and became an important industrial point of focus. An important concern of the pharmaceutical industry is to deliver the medicine to a specified tissue or bloodstream by taking the perfect route according to the physiological rules. Injection and oral administration are the most popular drug intake methods. In contrast, for certain therapies, these aforementioned methods are not suitable, especially for new therapeutic agents that need a specific delivery system like unstable drugs, proteins, nucleic acid, and poorly soluble drugs. This problem was solved at the range of nanoscale by “nanotechnology” which gave scientists the opportunity to discover and investigate a wide range of novel materials. Nanotechnology encompasses a wide array of technological concepts with high application potential [1].

Drug delivery systems (DDS) are a subgroup of nanoparticles that are designed with an aim to increase the therapeutic efficiency of drugs. Many problems come along when taking into account the delivery of drugs to a designated tissue or cell but these problems are overcome by using several drug delivery systems [2]. For this purpose, DDS uses mesoporous materials. Stimulated mesoporous materials that show physiochemical responses are being studied to discover if they could act as potential drug delivery systems. These materials can be stimulated by changing the environmental parameters such as temperature, pH and electric field [3].

As a result of their wide internal surface area, mesoporous inorganic solids ($\sim 20\text{--}500$ Å) have been used as sorption medium, also, they are used as catalysts. The microporous materials typically are solids with a crystalline frame, (e.g., zeolites). However, metallo-phosphates can have pores as large as $\sim 10\text{--}12$ Å, while mineral cacoxenite can have pores that measure ~ 14 Å. Modified layered materials and silicas are examples of mesoporous solids that are usually found to be amorphous or paracrystalline in nature, with pores having irregular distribution and size variation. In order to control the pore size, silicate layers are inserted as surfactants. However, the original material with a layered structure is still present in the final product. In the presence of the surfactant, calcinated aluminosilicate gels can be synthesized to create mesoporous solids. By choosing the suitable surfactant, uniform pores

with dimensions ranging between 16 Å-100 Å can be formed within the material. The efficiency of the surfactant depends on reaction conditions and used chemicals. An explanation for the underlying mechanism of the creation of such mesoporous materials is given as the formation of a scaffold by the arrangement of liquid-crystal molecules, where the surfactant micelles are separated by inorganic walls of silicate material [4].

In the last few years, the unique pore volume and size of mesoporous silicas (MS) with a high surface area, have allowed them to be drug delivery controlled carriers with a wide range of applications. Mesoporous silicas show a higher ability for loading drugs and controlled drug release compared to amorphous colloidal and porous silica [5].

The ideal drug delivery system includes; improvement of the drug absorption, enhancement of drug stability, allowing to target the drug for its specific tissue in addition to controlling the release of the drug. DDSs are preferable to be composed of biodegradable materials that permit its removal through metabolic pathways [6]. Nanotechnology is the nanoscale control of matter by formation and using systems, materials, and devices [7]. Practically, this technology interested in the formation of the biocompatible Nano-carriers therapeutic materials (e.g., Nanocapsules, nanoparticles (NPs)) [8].

During the latest few years, MSNs (i.e., mesoporous silica nanoparticles) garnered attention among scientists for their biomedical applications as effective scaffolds in the DDS. The properties of MSNs (i.e., surface, size, morphology, and structure) are easily changeable for drug delivery and release controlled drug loading, and multi-functionalization purposes. In 1992, a group of scientists discovered a novel ordered mesoporous silica (MS) i.e., the MCM-type-41. Such discovery enabled researchers to benefit from the MS controlled applications and syntheses [9].

According to **Duaa Mohammed Tariq (2012)**, drug delivery process has a significant effect on its efficiency and there is an increasing need for improving new routes to increase the effectiveness of the drug release, including which is the use of mesoporous carriers in drug delivery systems. Furthermore, according to **Al Mamori, Feras Falih (2011)**, drug doses in the form of tablets, capsules are usually coated with polymeric films without which the dose may be dissolved completely in the stomach causing an increase in the risk of toxic side effects of the medicine [10]. Also, **Rehan Mohammad (2014)** mentioned that

Nanoparticles are perfect candidates in terms of carrying therapeutic drugs only to the targeted organ tissues. These particles reduce the side effect and have an increased efficacy as a result of their tiny size which enable them to penetrate efficiently to individual cells through small capillaries across the barriers. Moreover, their tiny size allows releasing drug at the targeted cells efficiently. After they complete their action, they degrade into nontoxic products like H_2 , N_2 , and H_2O and are ejected from the body. **From these previous studies**, we conclude that we have an important cause in controlling the kinetics of drug release to enhance the medicine dosage effectiveness [11] [12] [13].

Every day a lot of drugs are discovered to treat numerous diseases that human beings suffer from. These discoveries are accompanied with many studies for the DDS to improve the drug absorption effectiveness and drug's therapeutic efficiency. Studying mesoporous materials and their role as carriers for therapeutic drugs is considered to be the most important study that is needed for drugs of low solubility and for drugs that are affected with the conditions of the stomach [14] [15].

The aim of this study is to investigate ways to control drug delivery systems obtained by mesoporous drug carriers and also to study the nature of such materials, their properties, suitability for various drug types. In addition, it is also aimed to study the effectiveness of mesoporous materials in delivering the drug to the targeted tissue in order to increase the therapeutic efficiency of the drug.

1.1.THE MESOPOROUS MATERIALS

1.1.1. What are nanoparticles (NPs)?

Nanoparticles are defined as solid particles with a size range from 10 to 1000nm to which drug is entrapped, dissolved, attached or encapsulated. Nanocapsules, nanospheres or nanoparticles are synthesized with different preparation methods. In nanocapsulated systems, a membrane of unique polymer surrounds a cavity that confines the drug. In nanospheres, the drug is uniformly and physically dispersed within the internal matrix [16-19].

Nanoparticle design aims to control surface properties and sizes of nanoparticles in order to increase the drug effectiveness by making it so that the active agents are released at a designated location within the body at a desired dose and rate. Liposomes are good drug carriers because

of their unique characteristics such as the ability to target the desired infected cells, decrease the toxicity of the drug (i.e., side effects) and decrease the drug degradation.

Despite these abovementioned advantages, applications of liposomes are limited due to their poor encapsulation efficiency. In the presence of blood components, water-soluble drug rapidly leaks and the liposomes become less stable. In contrast, are the nanoparticles, it offers some unique advantages that don't exist in liposomes as they help to increase the proteins or drugs stabilization then controlling the proteins or drugs releasing properties [20][21].

Table 1.1: Liposomes and Nanoparticles properties summary.

Liposomes	Nanoparticles
Target the infected cells	Great ability to target the infected cells
Decrease toxicity and side effects and degradation of the drug before reaching the targeted infected cells	Decrease toxicity and side effects and degradation of the drug before reaching the targeted infected cells
poor encapsulation efficiency	Increase in encapsulation efficiency
Poor stability	High stability
Limited release properties	Unlimited release properties

The “DDS” that uses nanoparticles main advantages

1. The ability to change the nanoparticles surface characteristics and particle size to have the maximum benefit of the drug after parenteral administration.
2. Controlling the drug release at targeted cells in addition to the transportation phase, changing the drug distribution in the organ then help to release the drug from the system to enhance the therapeutic effectiveness of the drug while reducing side effects.
3. Controlling the characteristics of release and degradation of the nanoparticle by a good choice of matrix constituents.

4. A drug can enter the system without going through chemical reactions which preserve the drug from the degradation and increases drug loading.
5. Aiming for the infected cells could be easily accomplished by using magnetic guidance or attaching the particles surface with targeting-ligands.
6. A wide variety of carrier particles used for different types of administration including nasal, oral, intra-ocular, parenteral.

NPs usage limitations

1. The aggregation between particle to particle can happen because of the larger surface area and smaller size, making the handling of nanoparticles physically hard in dry and liquid forms.
2. Limitation in burst release and drug loading because of the smaller size. However, this problem should be overcome before using the nanoparticles clinically [22].

Classification of nanoparticles

- i. Nanoparticles are classified based on their dimensions into three groups [23].

One dimensional nanoparticles:

The structures that have one dimension between 1-100 nm are defined as one dimensional nanoparticle. Due to their characteristic features, scientists try to make new types of such structures or minimize the microstructures into the size of 1-100 nm [24].

Two dimensional nanoparticles:

The most widely known nanoparticles in classification are Carbon nanotubes.

Three dimensional nanoparticles:

Fullerenes (Carbon 60), Quantum Dots, Dendrimers, are known examples of three-dimensional nanoparticles [25].

- i. Other scientists classified nanoparticles into four classes related to their dimensions as the three aforementioned classes (i.e., one, two and three dimensional nanoparticles) in addition to the class of zero dimensional nanoparticles [26]

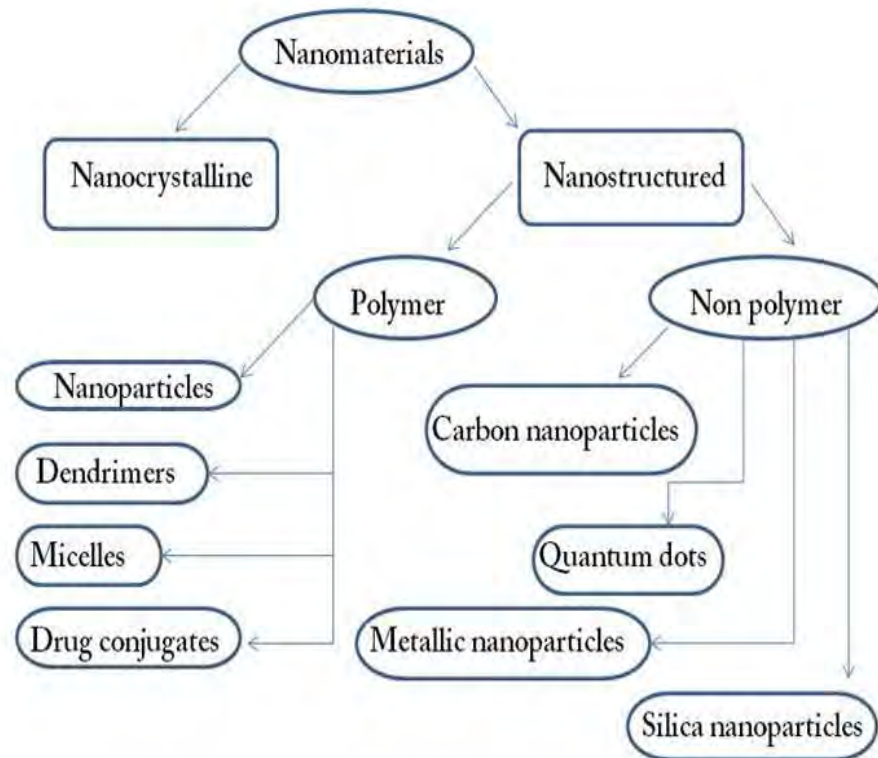


Figure 1.1: Various types of nanostructures [27].

ii. Classification of nanoparticles according to its size

- 1- Microporous: The pore diameters of these materials are 2 nm or less.
- 2- Mesoporous: The pore diameters of these materials are between 2-50 nm.
- 3- Macroporous: The pore diameters of these materials are 50 nm or more.

1.1.2. Characterization techniques of NPs

Surface charge, size, and morphology are the three properties with which nanoparticles are characterized. Characterization takes place by means of enhanced microscopic techniques such as FTIR, SEM, XRD, and TG [25].

FTIR “Fourier transform-infrared spectroscopy” Techniques are applied widely to achieve absorption in the spectrum of IR and issue three different states like solid, liquid and gases. This technique is used to characterize the nature of surface adsorbents in nanoparticles [28].

SEM “Scanning electron microscopy” Techniques work at Nano scale. Using SEM techniques, Scientists can study nanomaterials' morphology, as well as their dispersion within the matrix or bulk. This technique is based on the principle of electron scanning.

XRD “X-ray diffractometry” Techniques target characterizing the NPs structural properties as the most important technique of characterization. XRD not only gives the required information for the NPs crystallinity but also gives the required information for its phase. In addition, the formula of Debye Scherer roughly provides the NPs particle size [29] [30]. The XRD technique is able to identify multiphase NPs as well as single phase NPs [31].

1.1.3. Where are nanoparticles used?

The application of nanoparticles is unlimited due to the characteristic features that enable them to be used within different fields of science [32]. Nanoparticles are used in areas such as manufacturing, environment, energy, electronics, and medicine (e.g., Nickel NPs used in creating artificial skin, and photo-catalytic NPs of copper-tungsten-oxide, used to enhance the high reaction surface area for breaking down oil into biodegradable compounds).

1.1.4. Macroporous, mesoporous, microporous materials

The materials that contain cavities, channels or interstices are known as porous materials. The porous material properties change depending on the pores shape, size, composition, and arrangement of the material. In addition, their characteristics change depend on porosity (i.e., the ratio between the total relative pore volumes divided by the material apparent volume).

In the last few years, scientific researches concentrated on the adjustment of the shape and size of solids for different nanometer (nm) to micrometer (μm) length scales [33].

Researches worked on the porous materials concentrated on the differentiation in pore densities, sizes, and shapes but the most important features that attracted the attention was increasing in the surface area that increases the properties of adsorbent and absorbent [34][35].

A new porous material with different porous size is obtained by modifying the material surface. The pore size is the feature upon which the classification based. The classification of the porous materials according to IUPAC are (Micro- Meso- and Macro-porous) (Figure 1.2).

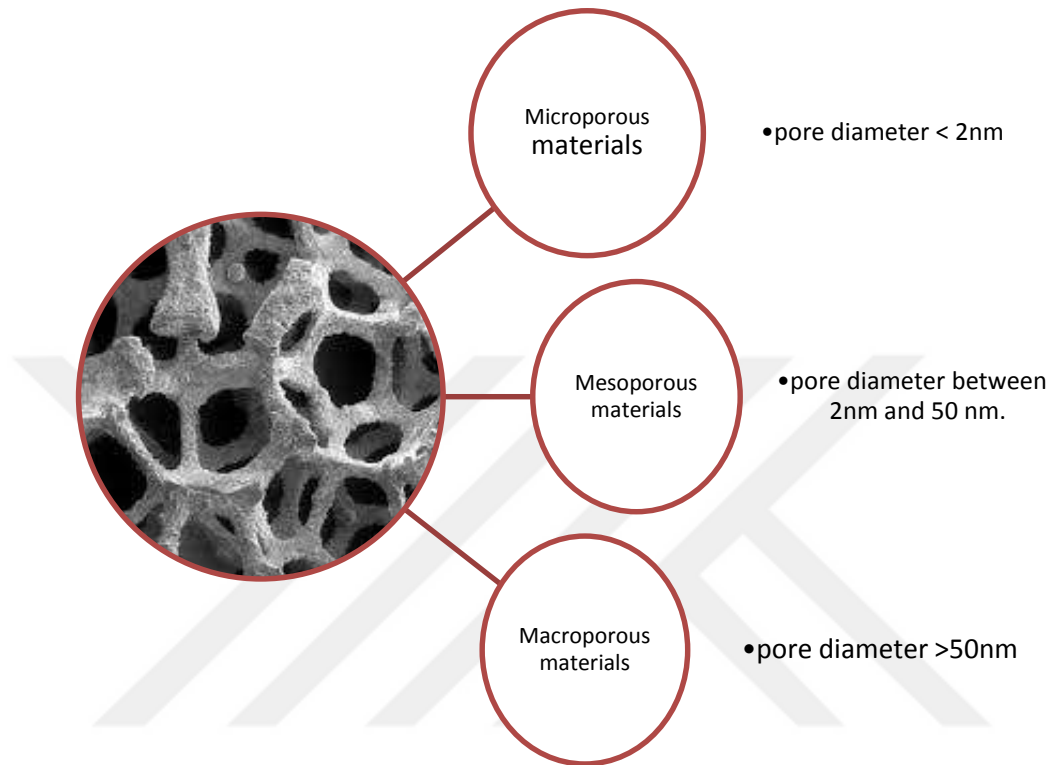


Figure 1.2: The porous materials and its diameter.

Such porous materials are made from substances such as silicon, carbon, ceramics, silicates, polymers, and minerals. Metallic nanoparticles coating for those porous materials might enhance the properties in terms of biocompatibility. The focused researches on silica-based materials concentrate on giving the porous material channels and walls with large active surface area, where the structure mix with metals functionally with aromatic or aliphatic groups and organic phases [34].

Organic compounds can be used to synthesize porous materials. Organic compounds through a route of versatile non-surfactant could act as agents for pore-formation, (sol-gel process). Such organic compounds (non-surfactants) were used in the preparation of porous materials. These non-surfactants are removed, when the process end, by solvent extraction [36]. Another way to obtain porous material is through using surfactants; these can be done by using the agents of structure-directing which controls the inorganic polymers development to different mesoscale

materials with different sizes and shapes. Various structures and components of porous materials, such as nanowires, nanoparticles, nanoporous and nanotubes materials, could be synthesized using simple chemical reaction and surfactant micelles through the structure controlling [37][38].

1.1.5. Definition of mesoporous materials

Mesoporous materials are defined according to IUPAC notation as pores between 2 and 50 nm in diameters contained in a material [39].

1.1.6. Synthesis of mesoporous materials

Different methods are used to synthesize NPs as generally shown in the next Figure [27].

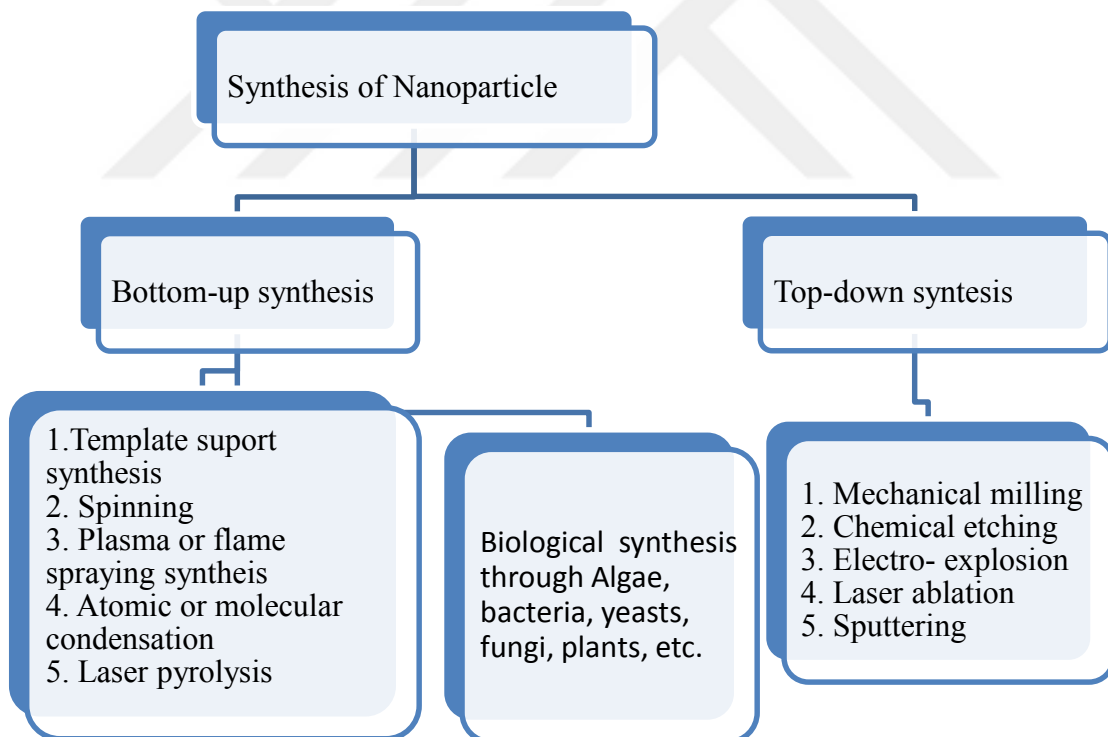


Figure 1.3: Nanoparticles different methods of synthetic.

Mesoporous materials are synthesized by bottom-up synthesis through template support synthesis. To illustrate, mesoporous inorganic oxides are a welcome supplement to crystalline zeolites (pore size up to 1.2 nm). When one reactant is too big or too hydrophobic to implement in the pores of zeolite a mesoporous catalyst will be used. The synthesis of mesoporous silicas by old techniques uses ionic amphiphiles with a low molecular weight as additives to direct the structure while if swelling agents are needed, inert oils are used.

1.1.6.1. Bottom-up synthesis

The NPs formation in this pathway is used in reverse order starting from relatively simple substances. In other words, a bottom-up synthesis approach can be called the approach of building up. Sedimentation and reduction techniques are examples of this case. It includes green synthesis, sol-gel, biochemical, and spinning synthesise “This technique graphene domains with TiO₂ anatase NPs” [40] [41]. Alizarin was offered TiO₂ with high binding capacity by the terminal groups of axial hydroxyl, that’s why it was selected as the photoactive composite synthesized precursors for photo-catalytic blue methylene degradation. The anatase form was confirmed by XRD pattern. SEM techniques indicated that as temperature increases, the size of NPs also increases. [42][43][44].

1.1.6.2. Top-down synthesis

It is called a destructive approach, as it starts from a large molecule that decomposes to multiple small particles then those particles are suitably transformed to NPs. Top-down synthesis method examples are physically vaped deposition (PVD), CVD, grinding/milling, and the different techniques of decomposition [37]. The NPs of coconut shell (CS) is synthesized using this approach. The raw CS powders milled finely with the planetary mill and the ceramic balls help. Regardless of the different techniques of characterization, increasing in the time leads to decreases the size of the NPs crystallite. Each incremental hour leads to fading in the brownish color which means that the NPs size has decreased [45].

1.1.7. Mesoporous silicate materials

Different nanocarrier drug delivery systems are based on platforms with organic origins such as dendrimers, liposomes, and polymers as carriers that could have, under some physiological conditions, release therapeutic agents. Nanoparticles like nanocrystals of gold semiconductor,

nanoparticles of superparamagnetic, in addition to silica-based and silicon materials had proven to be a promising drug delivery carriers [46]. Researchers have shown great attention to the Mesoporous silica nanoparticles (MSNs) because of their drug delivery systems field of applications as a promising potential. The materials of MSNs are solid with a porous structure like the honeycomb that contains many mesopores (i.e., empty channels) arranged as a planer network. Recent studies showed that the nanoparticles of MSNs have advanced biocompatibility for applications of pharmacological at suitable concentrations. However, compared to others (e.g., amorphous silica material), they have shown lower biocompatibility [47] [48].

Nanoparticles that are silica-based also show many structural advantageous and characteristic properties features, like stable mesostructure, pore volume ($>1 \text{ cm}^3 \text{ g}^{-1}$), pore diameter tuning from 2 to 10 nm, higher surface area ($>700 \text{ m}^2 \text{ g}^{-1}$), surfaces with double face functionality (i.e., interior pore and exterior particle faces), and morphology modifiability (controlling both size and shape of the particle). Consequently, the quality of drug loading is high enough because of their permitted pore diameter and larger surface area. The drug molecules diffusional release tuning to form a high mesoporous structure order at the required area to give rise to local biogenic concentration. Then the doses are decreased and any chronic or acute complications are prevented. Moreover, the pharmaceutical cargoes can be effectively protected by using the MSNs, such as imaging agents, drugs, oligonucleotides, and enzymes, from the early releasing or the harsh environment undesired degradation (e.g., the intestines and stomach) before it reaches the targeted destination [49].

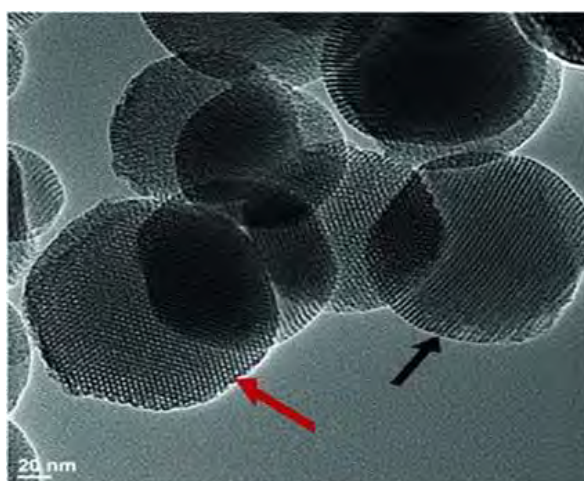


Figure 1.4: Nanoparticles of mesoporous silica image using (TEM).

1.2.DRUG DELIVERY SYSTEM

1.2.1. Definition of drugs

In general, drug is defined as a therapeutic agent that is different than food substance. Drugs used for disease diagnosis, protection, pacification, therapy or healing. In other words, the drug known as utilizing of a chemical component from any type in order to prevention, diagnosis or curative of any unhealthy condition and especially diseases, or as a component of a medication. Another definition for drug defined it as a hallucinogen or narcotic chemical substances in order to make certain effects in the central nervous system, which causes some behavior changes could lead to addiction often. For example, it is used to treat pain or induce anesthesia. The drug is also called medicine and have a definition of any taken substance through a cavity of the body, oral, in a skin blood vessel, or injected into a muscle to prevent or cure a disease. Also, any substance that could be abused for its effect as a depressant, stimulant, or hallucinogenic is called a drug.

1.2.2. What is “a drug delivery system”?

Controlled drug delivery systems (DDS) are viewed as the best DDSs as they have a few favorable circumstances over the customary types of known medications.

Liposomes, polymers, dendrimers, silicon or carbon materials, and attractive nanoparticles are the nanostructures that have been tried as carriers in DDSs.

Numerous pharmaceutical particles have been utilized as carriers in creating “DDS” running as customary tablet up to the level of utilizing created nanoparticles plan. NPs definitions are of kind particles that have particular characters, for example, the little size and tremendous surface territory which is joined by exceptional properties that bigger particles and mass materials don't have. It increases the bioavailability of different medications, extraordinarily the hydrophobic inadequately dissolvable medications, especially for drugs that cure tumors [50].

DDS is a multi-function and free field of research and is drawing in total consideration of pharmaceutical analysts, restorative specialists and industry. A safe and focused on DDS may upgrade the ways of some established drugs that are already used by patients, and also, it will

have an extraordinary impact in the advancement and achievement of new remedial techniques, for example, anticancer medication, peptide and protein drugs and quality treatment [8].

1.2.3. Need for controlled delivery system

As the number of diseases increases so does the need for inventing and discovering new tools to treat and manage them in an efficient manner. Besides the importance of finding the desired cure it is also necessary to determine the suitable dose and introduce it to the patients without any side effects or without making any complications to the patient.

For the past couple of years, an incredible consideration has been given regarding the improvement of novel drug delivery systems [51] [52]. There are numerous reasons behind this increased interest in these new systems. To begin with, acknowledgment of the likelihood of creating more efficient drugs by applying the ideas and strategies of controlled release drug delivery frameworks, along with their cost being too high to be suitable for cementation application has resulted in the conduction of further research on the amelioration of novel drug delivery frameworks [53].

Secondly, new drug delivery systems are expected to deliver peptides and proteins, to their target sides without bringing about any noteworthy immunogenicity or cell-mediated inactivation.

Thirdly, many medications and cancer treatments and treating catalyst lacking infections can be enhanced by using controlled DDSs. Finally, with the aid of conventional methods, drug efficiency can be enhanced by accurately targeting the cell or tissue of interest within the body, in this way diminishing both the size and number of measurements. If one somehow happened to conceptualize the perfect drug delivery framework [51] [52] [54].

1.2.4. Mesoporous materials for drug loading and drug delivery system

Over the most recent couple of years, the improvement of nanotechnology has inspired researchers to develop materials with nanostructures to be used in biomedical applications. In the 1990s, MCM 41 was integrated as an individual from the M41S atomic sifters group [4] [55].

Making the Mesoporous materials from surfactants supramolecular accumulation that layout the inorganic segment (ordinarily silica) in the amid union. After releasing the surfactant, generally by pyrolysis or disintegration with the appropriate solvent, the lattices of silica mesoporous become potential carriers for the drug [56].

Silica mesoporous materials have various features:

- a) A porous system that is exceptionally homogeneous in general and allows fine tuning of the drug loading and release properties.
- b) Pores with a high volume in order to transport the desired amount of drugs.
- c) High potential for adsorption of drugs as a result of high surface area.
- d) A surface with silanol-groups which permits better control over drug loading and release.

These features make mesoporous materials incredible drug carries for controlled DDSs, which gave rise to an increase in the number of researches conducted on them over the recent years.

Commercial DDSs which are generally obtained from novel polymers are exceptionally effective systems that are used in various fields. These systems additionally assist in a wide number of medicinal and therapeutic applications, for example, in odontology and orthopedics [58].

Mesoporous silica materials (e.g., DDSs) cornerstone advancement is the surface role or change using natural gatherings [59] [60].

It is possible to enhance such properties, for example by grafting organic silanes ((RO)₃ SiR'), functionalized surfaces using silanol groups (a high density Mesoporous silica) as illustrated in Figure 1.5.

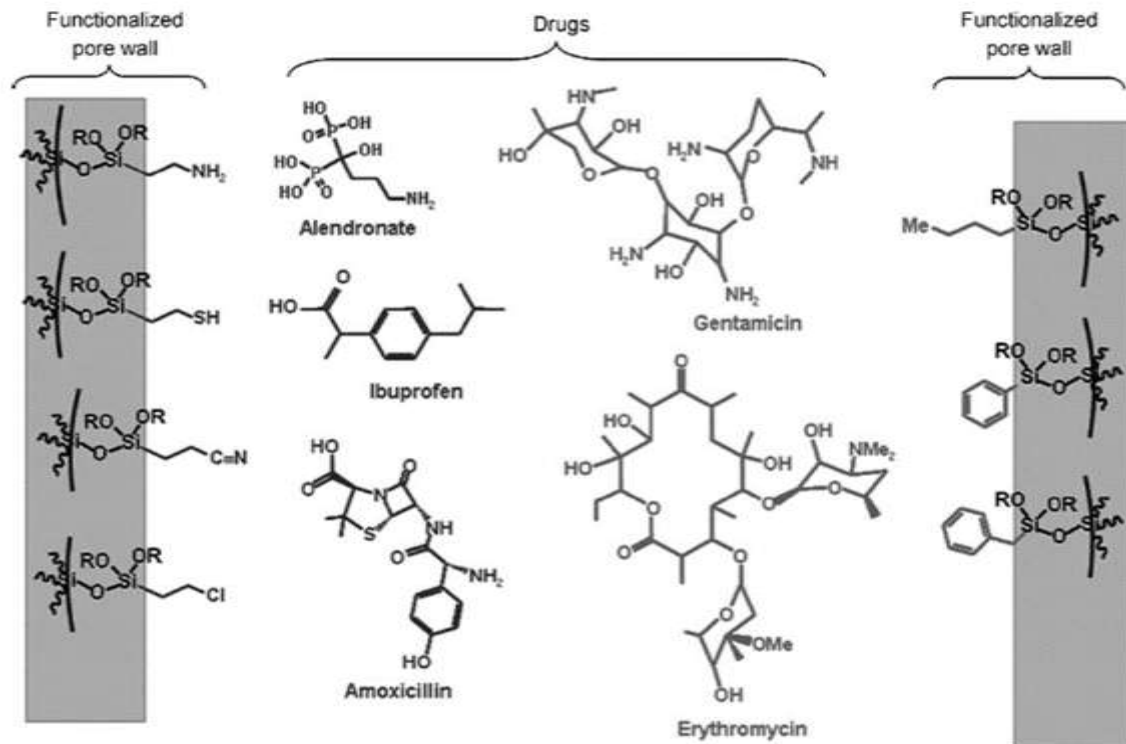


Figure 1.5: Silica mesoporous materials and their use in drug delivery systems.

Figure 1.5 shows one of the most frequently used drug delivery systems formed with silica mesoporous materials. While drug release can be efficiently controlled in many different ways, surface interaction is one of the strategies that is employed the most.

To increase their efficiency, the surface of mesoporous materials are functionalized with groups that can bind to drug molecules through ester groups or ionic bonds [61].

1.3.WHAT IS DRUG RELEASE?

Drug release is the process where the drug leaves the drug carrier following which it is absorbed, released into the bodily circulation, digested or discharged, during which it is pharmacologically active. Drug release can be done in various ways. Quick release drug carriers enable drugs to be released instantly without preventing or prolonging the disintegration or digestion of the carrier particles. Changed discharge dose shapes incorporate either delayed or prolonged. Delayed discharge is characterized as the discharged of a drug at a given moment rather than at the moment of deployment. Prolonged release drug carriers are used to produce drugs that are accessible after being deployed for a long period. Finally, controlled discharge

incorporates pulsatile and extended discharge materials. Pulsatile discharge is defined as the discharge of predetermined dosages of drugs at certain time intervals. For vitro disintegration, they have been perceived as the imperative component for improvement of drugs. Under specific conditions, drug release could be used as the way to bioequivalence. A few speculations/energy models portray medicate disintegration from quick and altered discharge measurements shapes. There are a few models to speak to the medication disintegration profiles while $f(t)$ is an element of time identified with the measure of medication broke down from the pharmaceutical dose framework.

The sort of medication, its polymorphic shape, crystalline, molecule size, dissolvability and sum in the pharmaceutical dose frame can impact the discharge dynamic. A water dissolvable medication consolidated in a framework is for the most part discharged by dispersion, where at lower levels of water solvent medication the grid self-disintegration would be the standard discharge system [62].

As of late, there has been expanded enthusiasm for materials of mesoporous silica to be used as controlling medication discharge carriers, by the drawn out issue addressing and medication organization higher control. Formless materials of mesoporous silica had been examined to have customizable pore measurement, nontoxic medication underpins nature in light, with plentiful bonds of Si-OH that give high pore surface region [63].

A few researchers have explored regular mesoporous silica materials (for example, MCM-41 and SBA-15) to be used as drug delivery frameworks [64] [65].

Up until now, just a small amount of articles were issued about boosts responsive medication discharge controlling from the type MCM-41 mesoporous silica [66].

1.3.1. The drug delivery systems commonly used polymers

Polymeric systems were utilized broadly in numerous applications in drug delivery, as particulate and dissolvable systems. Polymers could likewise be utilized for delivering drugs to particular destinations within the body as encapsulating materials. Particulate systems with regards to biodegradable polymers have as of late garnered some attention. A significant number of these frameworks depend on smaller scale particles produced using poly-lactide-co-glycolide or poly-lactide copolymers, albeit other materials, for example, poly (organo)

phosphazenes are also present. More recent microparticles used in drug research focused on the presentation of new copolymers as (ethylene-oxide) polymers, for example, poly-lactide poly (ethylene oxide). Suddenly, in fluid media, these micelle-like particles materials frame, while the produced center may embody a medication using the copolymer hydrophobic moiety [67].

1.4.RELEASE KINETIC THEORIES

1.4.1. Zero order

Perfect delivery of medications inside the human body should follow "zero-order kinetics". In the blood, the drug should remain the same as it is during its delivery. The release amount in zero order could be expressed as

$$Q = Q_0 + K_0 t \quad (1-1)$$

(Q: the drug release amount (expecting that a discharge happens as the drug disintegrates), Q_0 : the medication underlying measure in arrangement (the typical value for Q_0 equals zero), while K_0 : a zero-order release constant).

1.4.2. First order

The condition looks like the other rate law conditions, which determine the release rate at kinetics first order for a fixation angle (i.e., $C_s - C_t$) between a mass fluid and a static fluid layer beside the strong surface.

This model has additionally been utilized to depict assimilation and additionally end of a few medications, the arrival of the medication which took after first request energy can be communicated by the condition:

$$dC / dt = k_1 (C_s - C_t) \quad (1-2)$$

(k: a rate constant, and dC / dt : a concentration change rate compared to time). The integrated equation form is:

$$\ln [C_s / (C_s - C_t)] = k_1 t \quad (1-3)$$

$$\log C = \log C_0 - k_1 t / 2.303 \quad (1-4)$$

(k: the rate constant at first order, t: the time, and C_0 : the drug concentration initial value).

1.4.3. Higuchi model

The principal scientific model put to clarify to explain drug delivery under a network framework was proposed by Higuchi in 1961. First it was put for planar frameworks; afterward extended to various states of permeable frameworks. Higuchi was the main researcher who had proposed a state describing the medication arrival from a grid of insoluble as a period subordinate process foundation square root in view of Fickian diffusion. An exceptionally incredible consideration has been given to Higuchi condition which depicts tranquilize discharge. Also, for our insight, no exploration has been accounted for that there is a deviation has been accounted for from the perfect Higuchi discharge design.

$$Q_t = K_H t^{1/2} \quad (1-5)$$

(t: time in hours, K_H : the constant of Higuchi, and Q_t : the drug releasing cumulative amount at the time).

1.4.4. Peppas model

Korsmeyer-Peppas model expresses a straightforward relationship to depict the framework discharge of medication at the conditions of the polymers. In order to comprehend a medication discharging system, around 60% of information about medication discharging were submitted in the model of Korsmeyer-Peppas.

$$M_t / M_\infty = K_m t^n \quad (1-6)$$

(n: the discharge exponent, k: the constant of discharge rate, and M_t/M_∞ : the least amount of discharged medication at time t). The exponent n is used to recognize diverse discharge for around then hollow formed grids. In this model, the estimation of n describes the discharge system of medication [62] [68].

2. MATERIALS AND METHODS

2.1. MATERIALS

Three samples are prepared in this work as scaffolds to study the usage of these samples in the drug release and delivery systems. The chemicals used in this work are given below:

Cetyl-trimethylammonium bromide

The first mesoporous nanoparticle used in the experiment was prepared using cetyl-trimethylammonium bromide (CTAB) also known as Cetrimonium bromide and was acquired from MERCK company. This compound has a chemical formula $C_{19}H_{42}BrN$ with a molecular weight of 364.45g/mol. It has the following chemical structure:

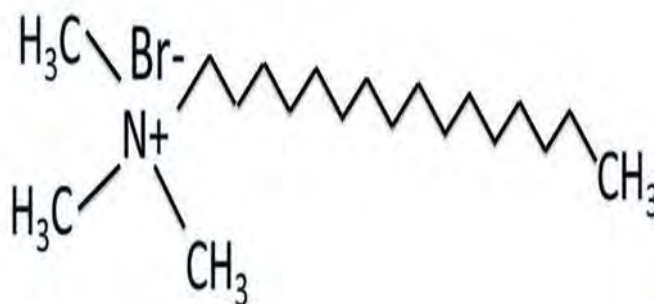


Figure 2.1: Chemical structure of cetyl-trimethylammonium bromide.

Tetraethylorthosilicate

Another compound used in the experiments is Tetraethylorthosilicate (TEOS), which was obtained from MERCK Company. This compound has the chemical formula $(C_2H_5O)_4Si$ and a molar mass: 208.33 g/mol with the following chemical structure:

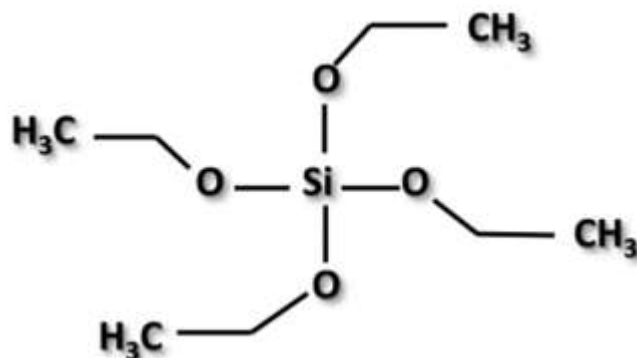


Figure 2.2: Chemical structure of Tetraethyl orthosilicate (TEOS).

Ammonium hydroxide (NH_4OH) was obtained from SIGMA ALDRICH.

5-Fluorouracil

5-Fluorouracil commercialized under Adrucil[®] trade name was used as one of the experimental drugs. It is used in chemotherapy as an anti-cancer drug (cytotoxic or antineoplastic).

5-Fluorouracil has been obtained from ALFA AESAR Company with 99% concentration. It has the chemical formula $\text{C}_4\text{H}_3\text{FN}_2\text{O}_2$ with molecular weight of 130.077g/mol and has the following chemical structure:

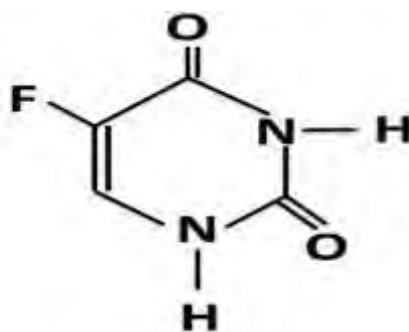


Figure 2.3: Chemical structure of Fluorouracil molecule.

Ciprofloxacin

The other model drug used in this work is Ciprofloxacin which is a fluoroquinolone-type antibiotic. Ciprofloxacin can also treat certain types of plague or anthrax related infection. It was obtained from XIAMEN Fine chemical import and export Co.Ltd Company. The chemical

formula of Ciprofloxacin is $C_{17}H_{18}NF_3O_3$ and its molecular weight is 331.346 g/mol. The chemical structure is as follows:

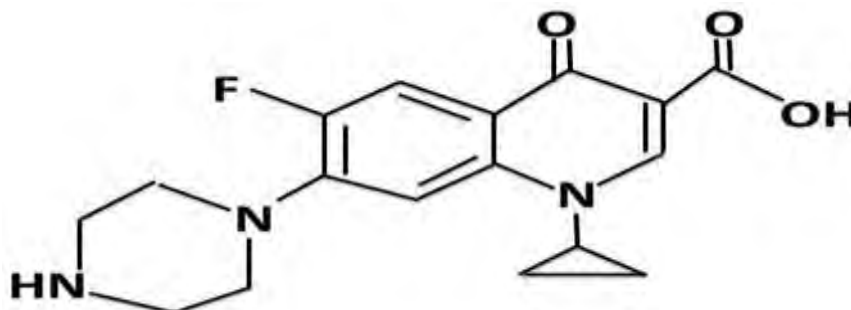


Figure 2.4: Chemical structure of Ciprofloxacin.

TritonX-100

TritonX-100 is the common name of Polyethylene glycol p-(1,1,3,3-tetramethyl butyl)-phenyl ether. Its chemical formula is $C_{20}H_{34}O_4$ and was obtained from ACROS ORGANICS. This compound has the molecular weight of 338.482g/mol and the chemical structure of TritonX-100 is shown in Figure 2.5:

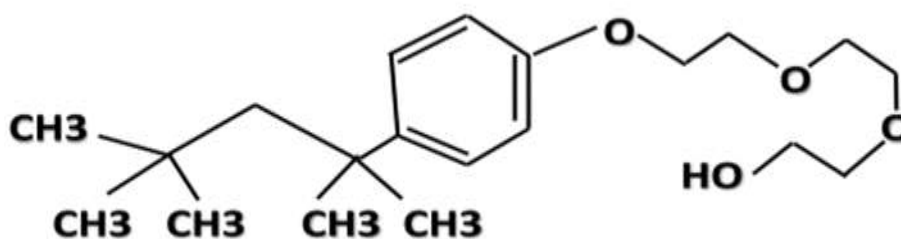


Figure 2.5: Chemical structure of (TritonX-100).

Polyoxyethylene sorbitan monostearate Polysorbate 60

Polyoxyethylene sorbitan monostearate Polysorbate 60 also known as Tween 60 was obtained from ACROS ORGANICS. It has the chemical formula $C_{35}H_{68}O_{10}$ and its molecular weight is

1309 g/mol. Tween 60 (oil-in-water co-emulsifier) is used for decorative cosmetics, skin care, and hair care. Tween 60 is used in creams, gels and cleansing products.

The products of Span Series such as polyoxyethylene derivatives surfactants include the Tween Series surfactants. Tween surfactants in inorganic liquids are soluble with varying degrees, dispersible or soluble in water, and are considered hydrophilic. Their usage are mainly in personal care applications.

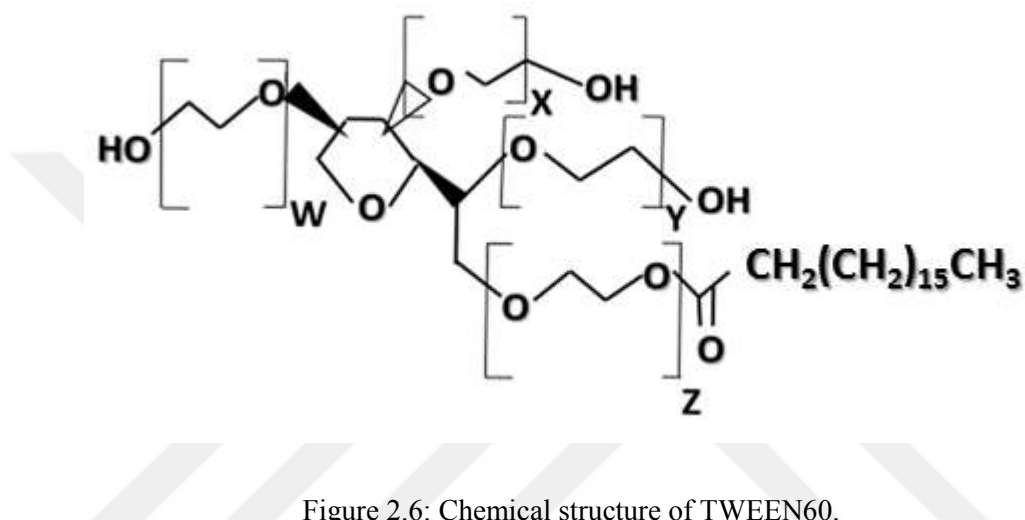


Figure 2.6: Chemical structure of TWEEN60.

Polyethylene glycol-sorbitan monooleate (Polysorbate 80)

Polyoxyethylene sorbitan monooleate, also known under the name of Polysorbate 80 and Tween80; was obtained from ACROS ORGANICS. It has the molecular formula $\text{C}_{32}\text{H}_{60}\text{O}_{10}$ and its molecular weight is 604.822 g/mol.

2.2.INSTRUMENTS:

The following instruments were mainly used in this work:

1. UV-VIS spectrophotometer.
2. FT-IR instrument
3. SEM instrument
4. Sputter Coater
5. XRD instrument

2.2.1. UV-VIS spectrophotometer

T80 UV-Vis instrument used in this work is a double beam high-performance spectrophotometer with a variable (0.5, 1, 2, 5nm) or fixed (2nm) spectral bandwidth.



Figure 2.8: UV-VIS spectrophotometer.

2.2.2. FT-IR instrument

FTIR instrument is used to examine the compounds by using infrared beams to characterize the functional groups for different chemical compounds. FT-IR spectra of the samples were studied with “Nicolet iS10/Smart iTR”. It works at wavelength ranges from 400- 4000 cm^{-1} .



Figure 2.9: FT-IR Instrument.

2.2.3. SEM instrument

It is an instrument used to characterize the morphological structure of the samples. Different types of samples showing the finite formations of these surfaces. The instrument used in this work was ZEISS EVO/ LS10.



Figure 2.10: SEM instrument.

2.2.4. Sputter coater

Sputter coater is used to cover the samples with gold to obtain a viable images with the SEM instrument. This instrument was manufactured by Quorum Company.

The conditions for coating which were used in the experiment 15 mA, 2 m Bar, and under an environment of Argon gas.



Figure 2.11: sputter coater.

2.2.5. XRD Instrument

XRD experiments were performed by using Philips XRD instrument PW 1730 model with Cu $K\alpha$ radiation including Ni filter and 36Kv potential, 20mA current goniometer rate is $2\theta=0.05/\text{min}$. It can be used with standard and high-temperature furnace units. X-Ray Diffraction (XRD) varies the X-Ray beam incidence angle in order to obtain reflected interference patterns which correspond to the lattice structures.



Figure 2.12: XRD Instrument.

2.2.6. BET Analysis

BET (Brunner-Emmett-Teller) method was used for estimation of specific surface area of the samples and pore size distribution was estimated by the Burrett-Joyner-Halenda (BJH) method using Quantachrome Instruments quadrasorb SII model. The pore volume of

mesoporous structures was calculated from the amount of Nitrogen adsorbed at certain p/p^0 value. The degasification process continues 20h at the temperature 100°C .

2.3.METHODS

2.3.1. Synthesize of mesoporous silica nanoparticles (MSNs)

Three “Mesoporous Silica Nanoparticles” (MSNs) have been synthesized successfully.

Preparation of BMM: The first sample was synthesized as follows: 1.31g of the surfactant cetyl-trimethylammonium bromide (CTAB) was totally dissolved in 52ml of distilled water in order to obtain a clear solution. In the next step, 4ml of Tetraethylorthosilicate (TEOS) as a source of silica gel was added into this solution while stirring. Then, 4ml of NH_4OH was added drop-wise to the mixture. The mixture was stirred for three hours continuously to obtain a white-colored gel. In the next step, the precipitates were filtered, washed, and dried for 3h at 120°C . Then, the solid was calcinated at (550°C for 5h) to remove the surfactant. The heating rate of the calcination process was $5^\circ\text{C}/\text{min}$ starting from room temperature until reaching 550°C . The resulted sample was marked as BMM. To recognize the physical, chemical properties of the prepared sample, FTIR, XRD and SEM studies were performed [69].

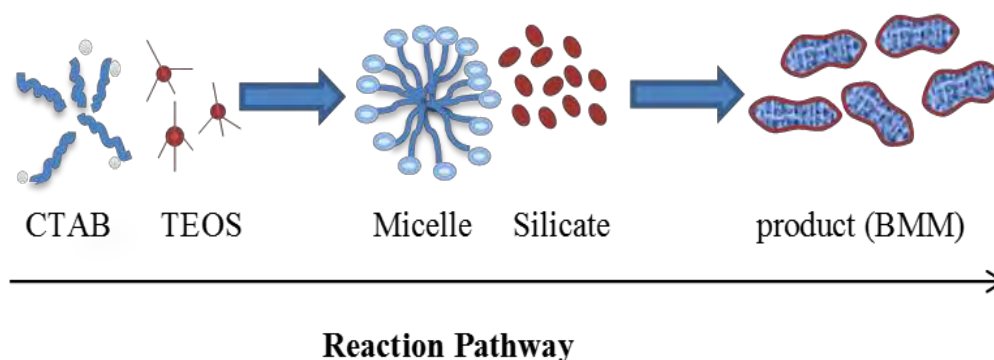


Figure 2.13: BMM synthesized schematically.

Preparation of TWN60 and TWN80: The second and third samples (MSNs) were prepared by mixing 3.2g of TritonX-100 with 0.583g of Tween60 and 0.583g of Tween 80 separately. 150g of distilled water was added into these two mixtures under stirring at $35\text{--}40^\circ\text{C}$ until a

transparent solution of the mixtures were obtained. The surfactants TritonX-100, Tween60 and Tween80 were used as non-contaminating auxiliary coordinating agents. In the following step, 8.4g of TEOS was added to both solutions. Then the mixtures were stirred for another 3h to get sol component. These steps were followed by adding 0.0415g of sodium fluoride to the sol-mixtures to obtain the gel component. The next step was to let the two gels age at room temperature for 24h. The solid products collected via filtration were repeatedly washed with distilled water and dried overnight at room temperature. The samples were then dried 24h at 50°C again. By using calcination process (450 °C for 5h with a heating rate of 10 °C/min), all the remaining templates were removed. The second sample remarked as TWN60 and the third sample remarked as TWN80 [70].

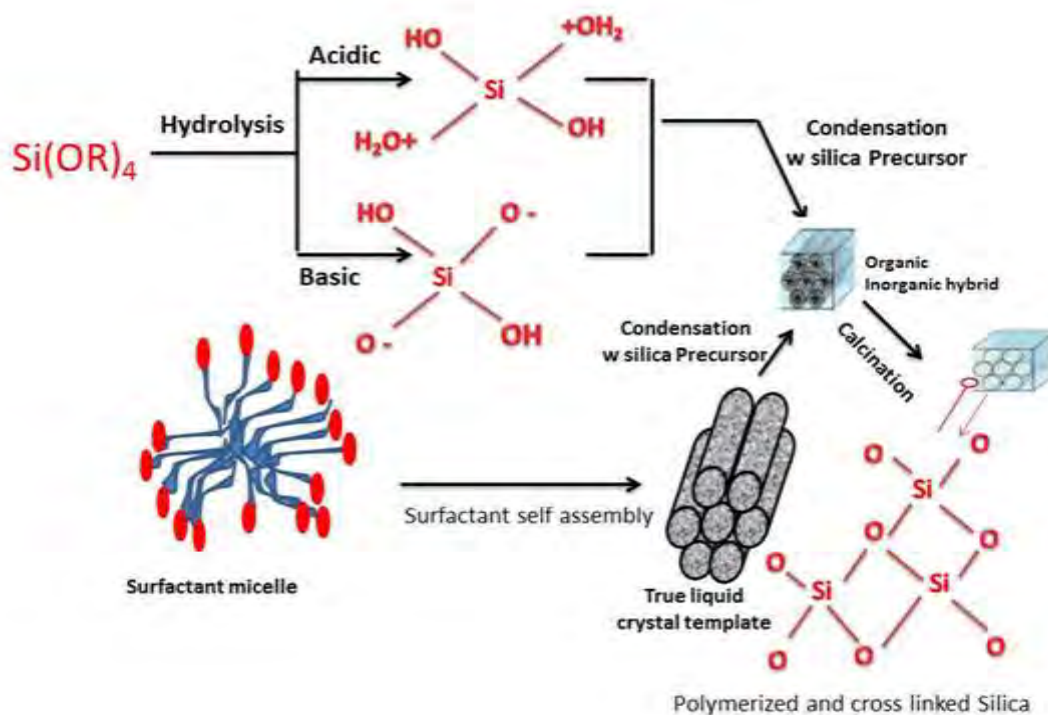


Figure 2.14: Synthesis steps of silica mesoporous.

2.3.2. Loading of 5-Fluorouracil and ciprofloxacin drugs

- 0.2g from BMM was added to 50ml of 5-Fluorouracil drug solution (20 ppm). The efficiency of drug loading with time was measured by using UV-vis spectrophotometer ($\lambda=266\text{nm}$).

- 0.2g from BMM was added to 50ml of Ciprofloxacin drug solution (1.5g/l). The efficiency of drug loading with time was measured by using UV-vis spectrophotometer ($\lambda=390\text{nm}$).
- 0.2g of TWN60 and TWN80 were added to 50ml of 5-Fluorouracil drug solutions (20 ppm) separately. The efficiency of drug loading was measured by using UV-vis spectrophotometer ($\lambda= 266\text{nm}$).
- 0.2g from TWN60 and TWN80 were added to 50ml of Ciprofloxacin drug solutions (1.5g/l) separately. The efficiency of loading according to time was measured by using UV-vis spectrophotometer ($\lambda=390\text{nm}$).

2.3.3. Drug release efficiency measurements

The samples were first loaded with the drugs then filtered, dried, and kept in 50ml buffer solutions as acidic pH= 2, neutral, and basic medium pH= 7.6 to measure the release with time by using UV-vis spectrophotometer. The release profile was studied by applying zero-order and first-order equations, Korsmeyer-Peppas and Higuchi kinetic models [71] [72].

All samples before and after drug loading were characterized by using FTIR, XRD, SEM instruments

3. RESULTS

3.1. FT-IR STUDIES

The samples prepared in this study were analyzed using FTIR spectra in order to make structural analyses and comparisons. Likewise, FTIR spectra of the drug active ingredients 5-Fluorouracil and Ciprofloxacin were first analyzed and their characteristic absorption peaks were identified.

3.1.1. FT-IR spectrum of TEOS

FT-IR spectrum was performed for pure TEOS and the result is shown in Figure 3.1.

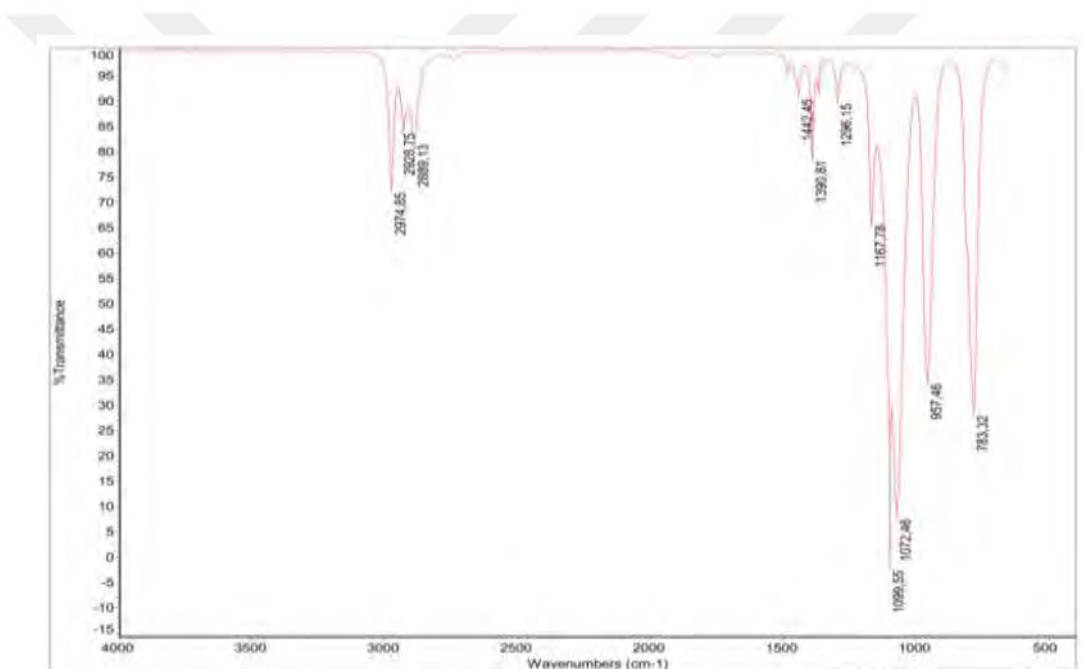


Figure 3.1: FTIR spectrum of TEOS.

3.1.2. FT-IR spectra of 5-Fluorouracil and Ciprofloxacin drugs

Figures 3.2 and 3.3 show the FTIR spectra of drugs containing 5-Fluorouracil and Ciprofloxacin respectively.

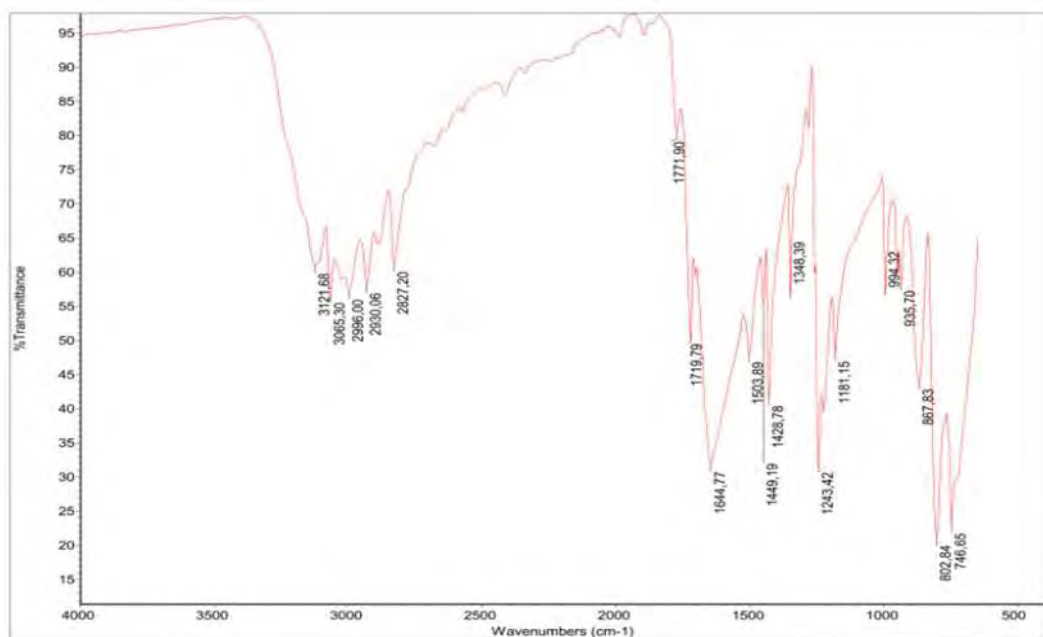


Figure 3.2: FTIR spectrum of 5-Fluorouracil.

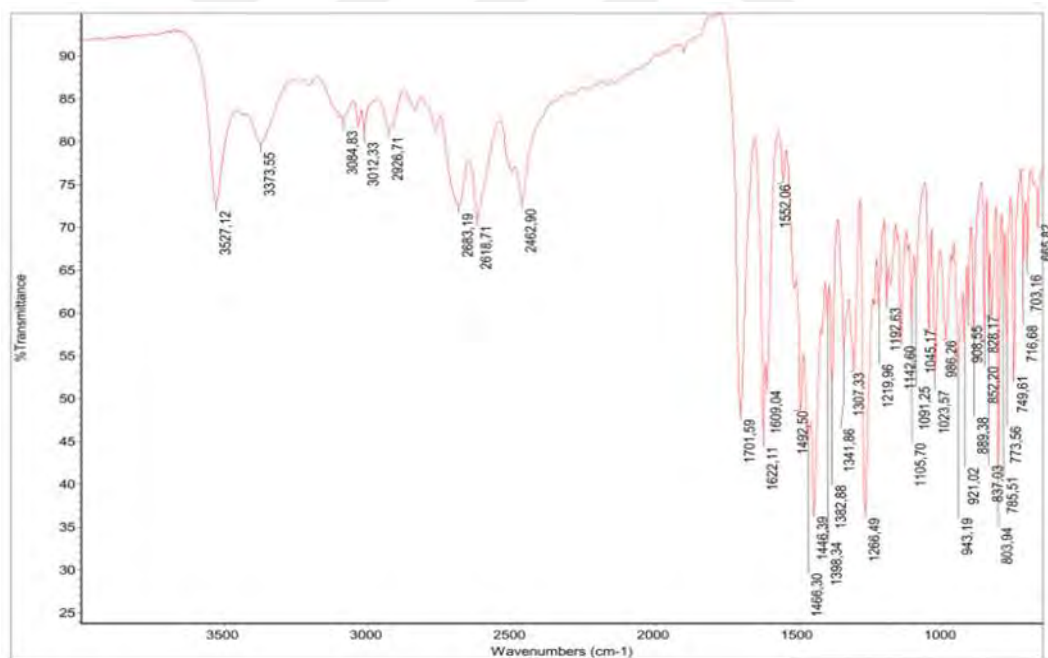


Figure 3.3: FTIR spectrum of Ciprofloxacin.

3.1.3. FT-IR spectra of BMM before and after calcination

The FT-IR studies of BMM before and after calcinations process were performed and the results are shown in Figures 3.4 and 3.5 respectively.

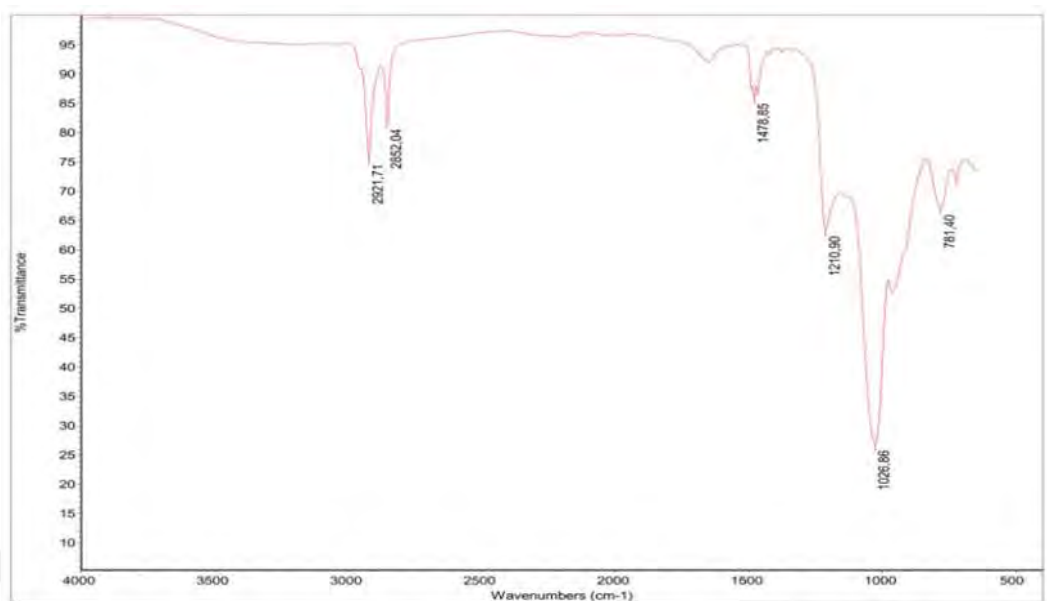


Figure 3.4: FTIR spectrum of BMM before calcination.

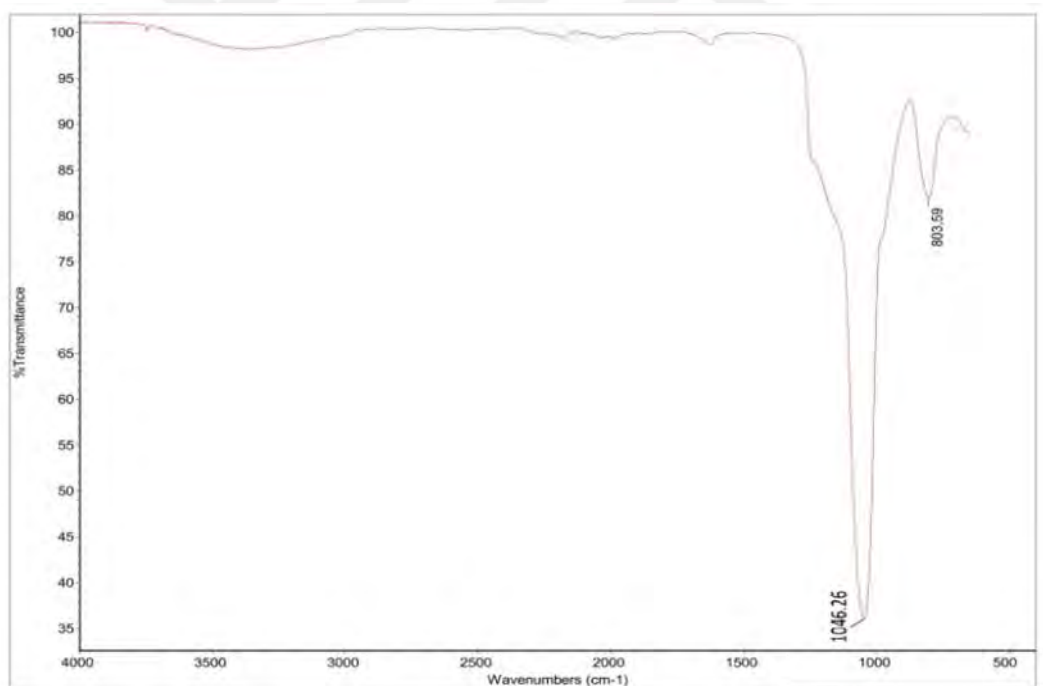


Figure 3.5: FTIR spectrum of BMM after calcination.

3.1.4. FT-IR spectra of BMM with drugs loaded.

FTIR studies of 5-Fluorouracil and Ciprofloxacin, loaded sample BMM were performed. The results were shown in Figures 3.6 and 3.7, respectively.

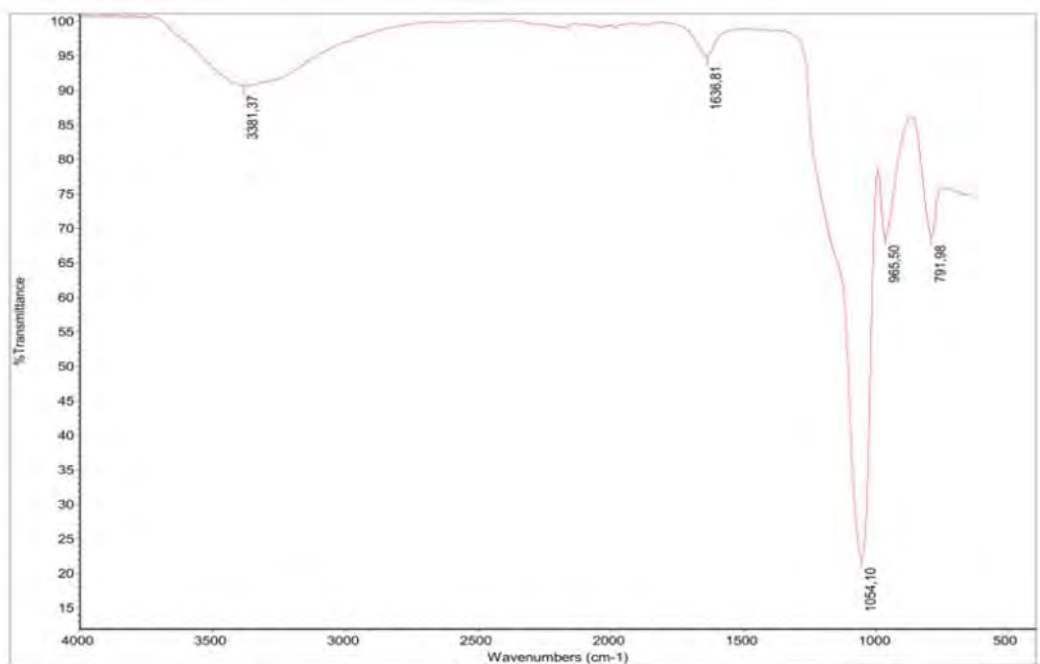


Figure 3.6: FTIR spectrum of BMM loaded with 5-Fluorouracil.

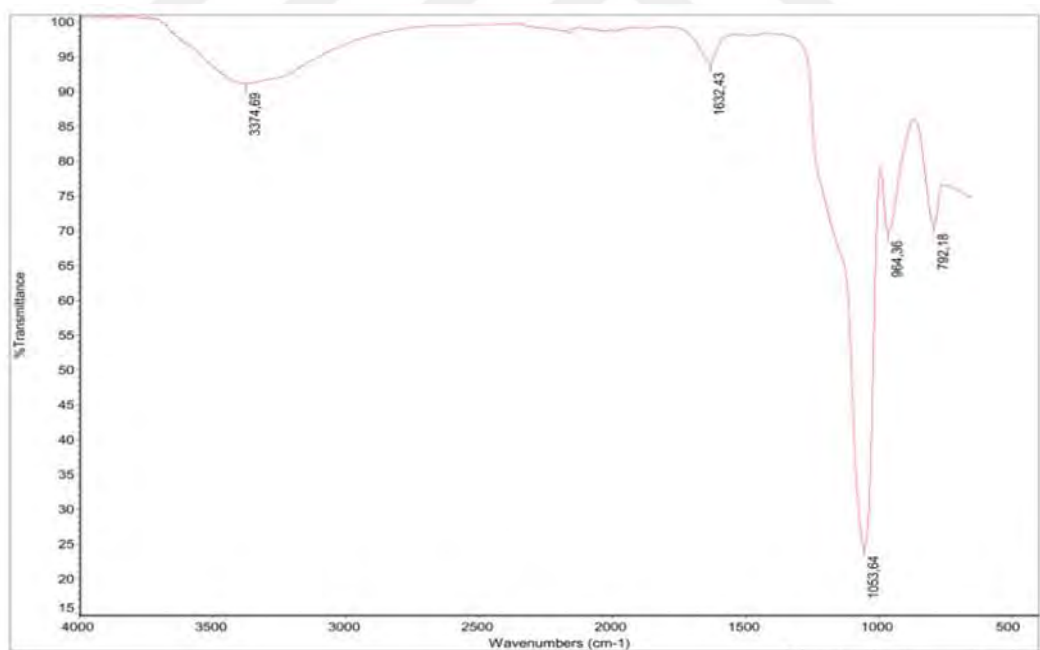


Figure 3.7: FTIR spectrum of BMM loaded with Ciprofloxacin.

3.1.5. FT-IR spectra of TWN60 before and after calcination

The results of FTIR studies for TWN60 before and after calcination were demonstrated in Figures 3.8 and 3.9 respectively.

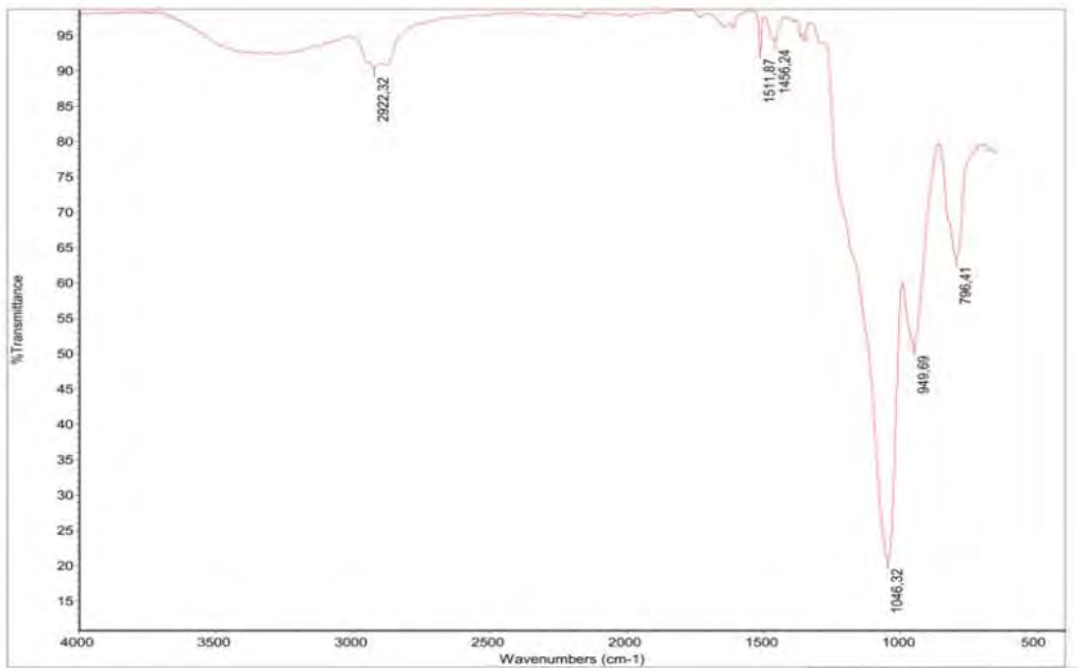


Figure 3.8: FTIR spectrum of TWN60 before calcination.

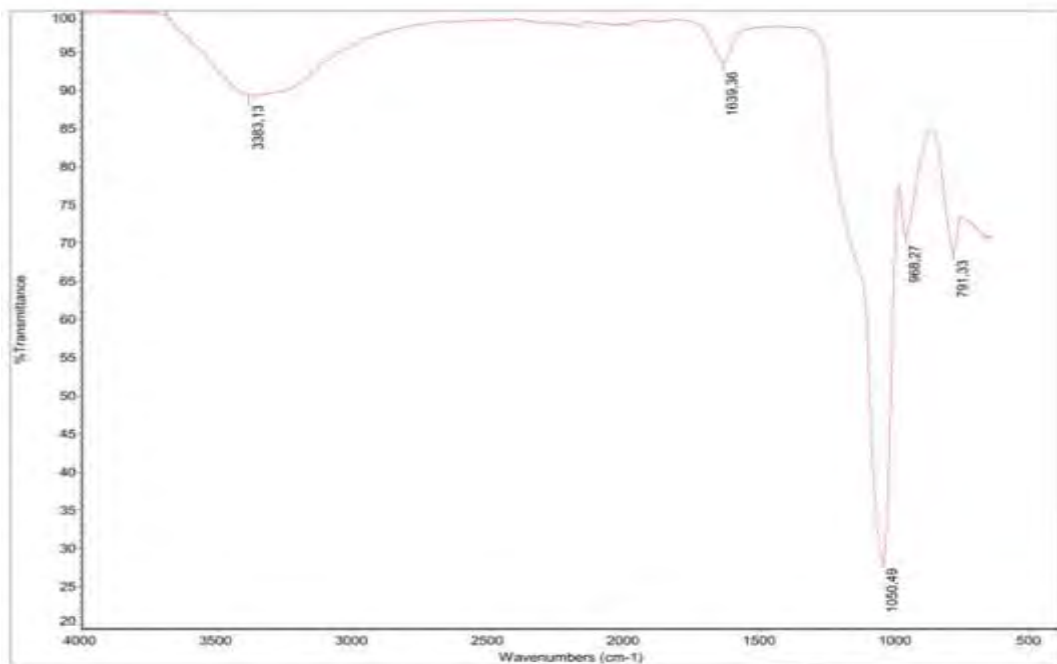


Figure 3.9: FTIR spectrum of TWN60 after calcination.

3.1.6. FT-IR spectra of TWN60 with drugs loaded

5-Fluorouracil and Ciprofloxacin were loaded into the TWN60. The results are shown in Figures 3.10 and 3.11, respectively.

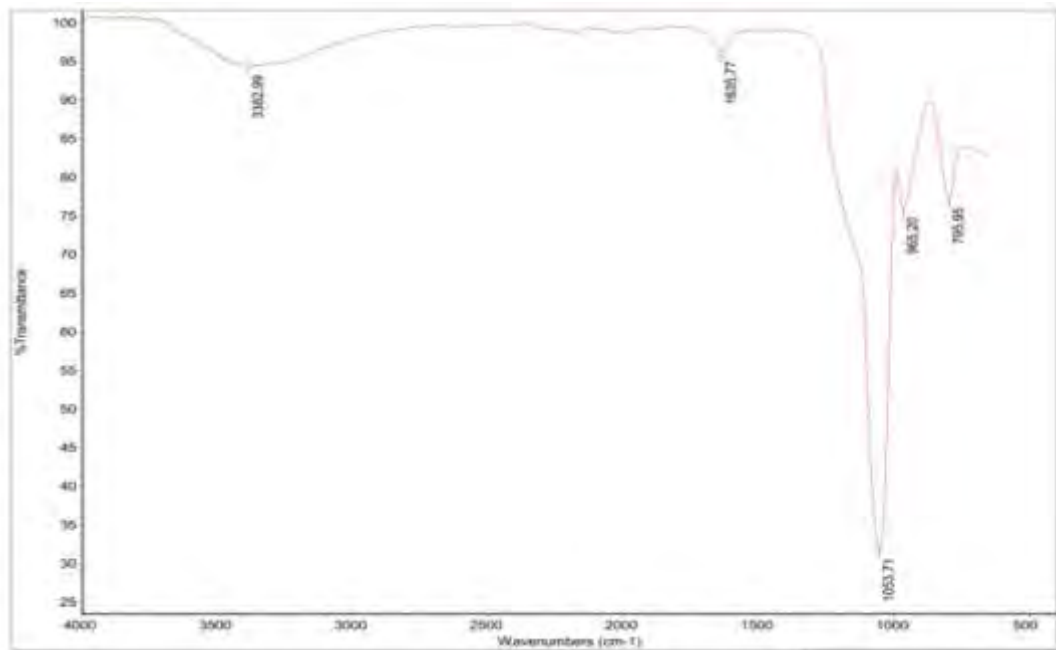


Figure 3.10: FTIR spectrum of TWN60 loaded with 5-Fluorouracil.

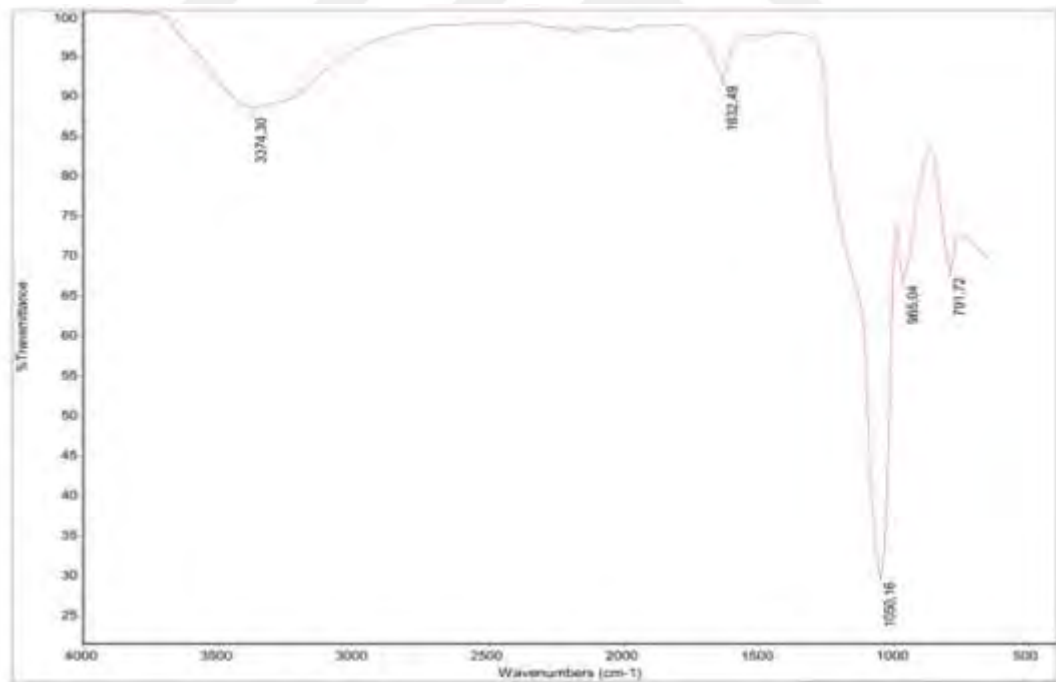


Figure 3.11: FTIR spectrum of TWN60 loaded with Ciprofloxacin.

3.1.7. FT-IR spectrum of TWN80 before and after calcination

FT-IR studies were performed also before and after calcination as shown in Figures 3.12 and 3.13, respectively.

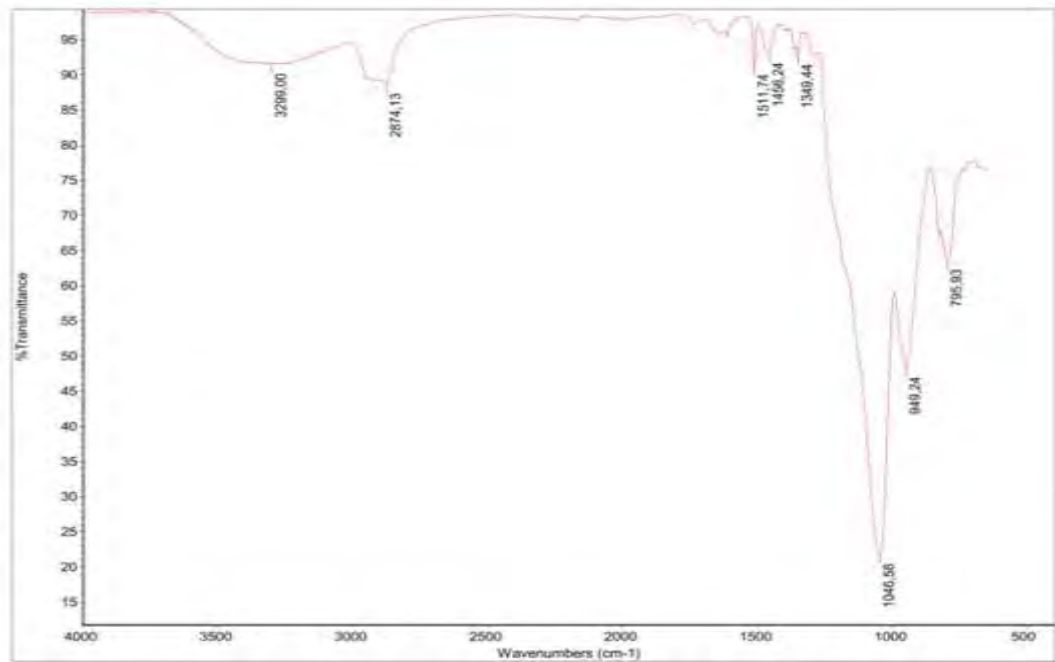


Figure 3.12: FTIR spectrum of TWN80 before calcination.

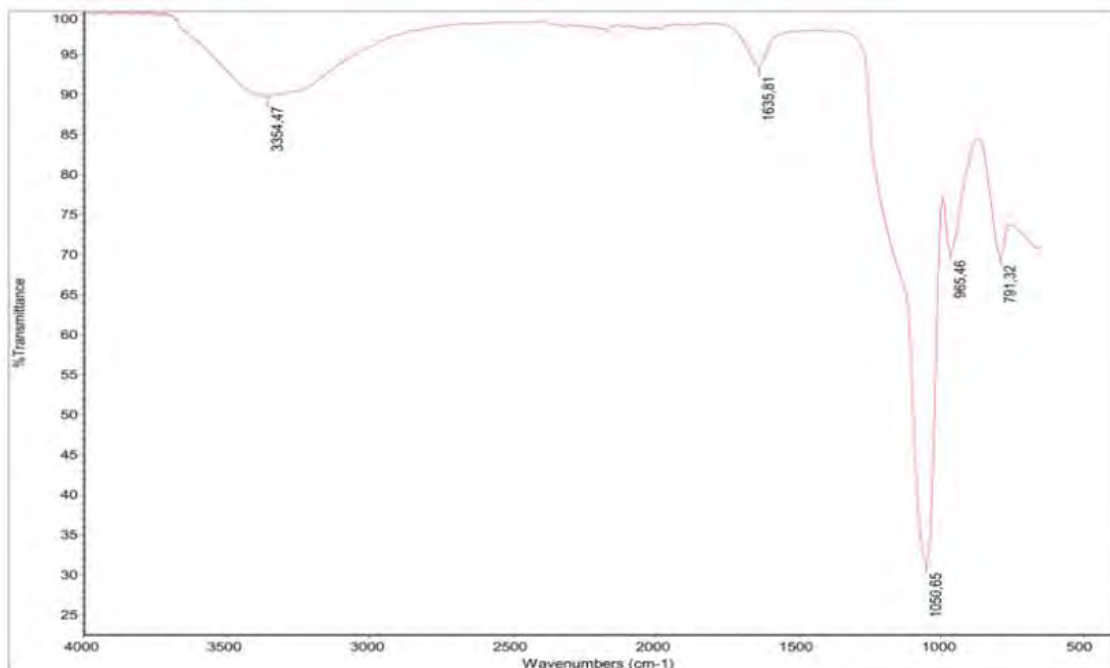


Figure 3.13: FTIR spectrum of TWN80 after calcination.

3.1.8. FT-IR spectra of TWN80 with drugs loaded

The results of FTIR studies of TWN80 loaded with 5-Fluorouracil and Ciprofloxacin are shown (Figures 3.14 and 3.15, respectively).

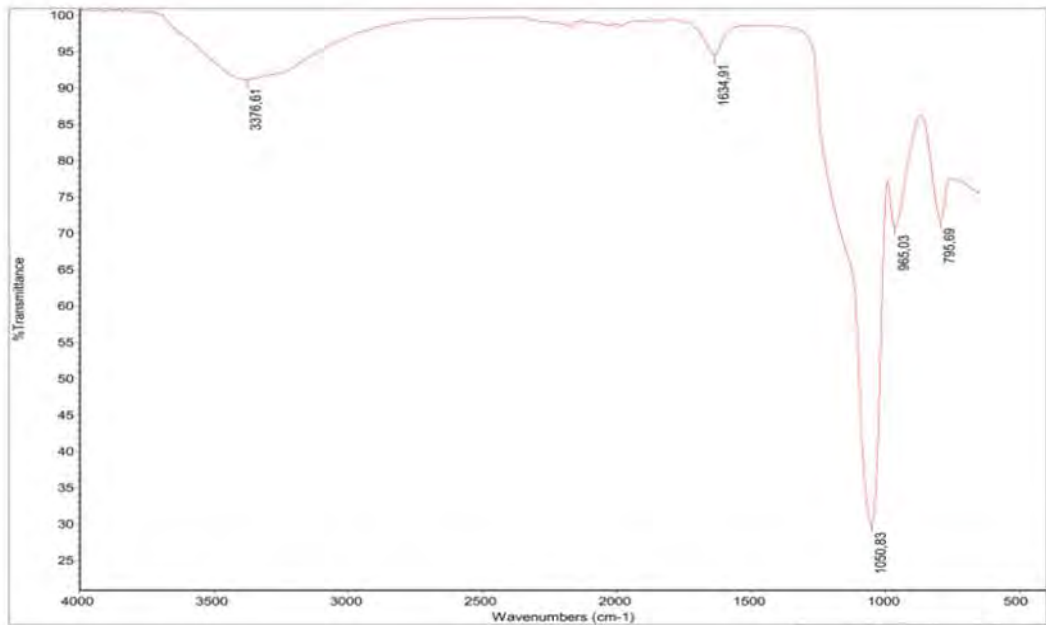


Figure 3.14: FTIR spectrum of TWN80 loaded with 5-Fluorourcil.

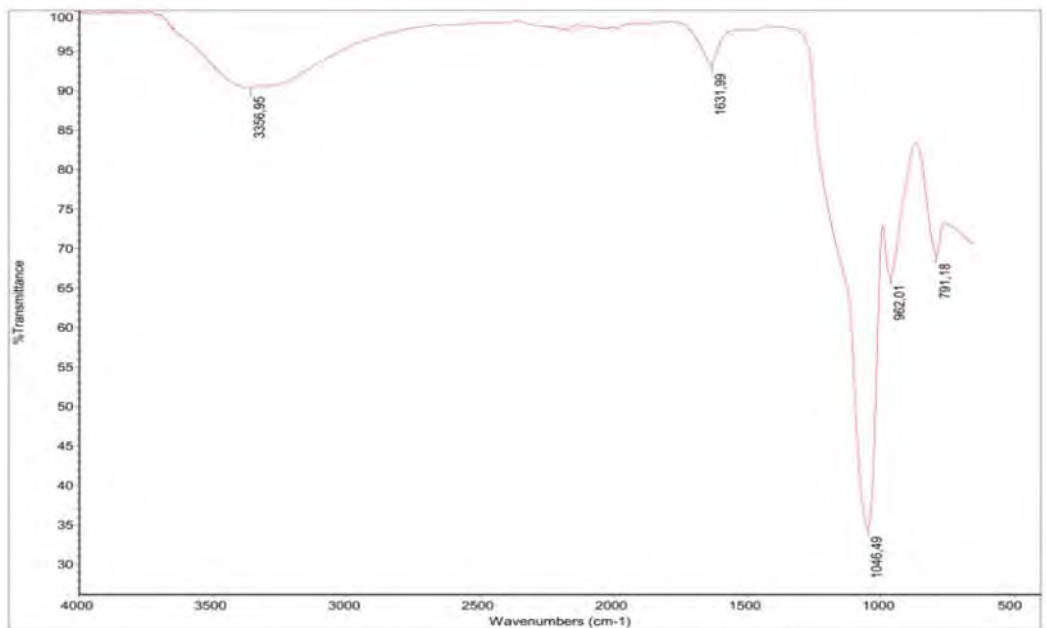


Figure 3.15: FTIR spectrum of TWN80 loaded with Ciprofloxacin.

3.2.SEM STUDIES:

Scanning Electron Microscope (SEM) is used to analyze the prepared samples and their micrographs were examined in order to assess their morphological features.

3.2.1. SEM micrograph of BMM

The results of SEM studies of BMM before calcination are shown in Figure 3.16.

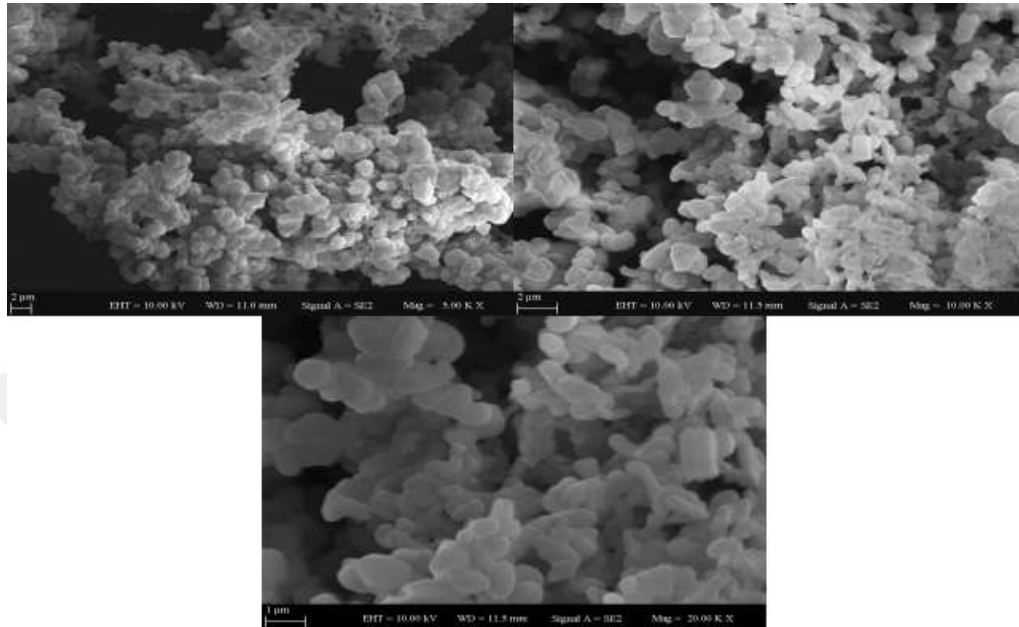


Figure 3.16: SEM micrograph of BMM before calcination.

After calcination, the SEM studies were performed again and we used the same magnification powers, the results are shown in Figure 3.17.

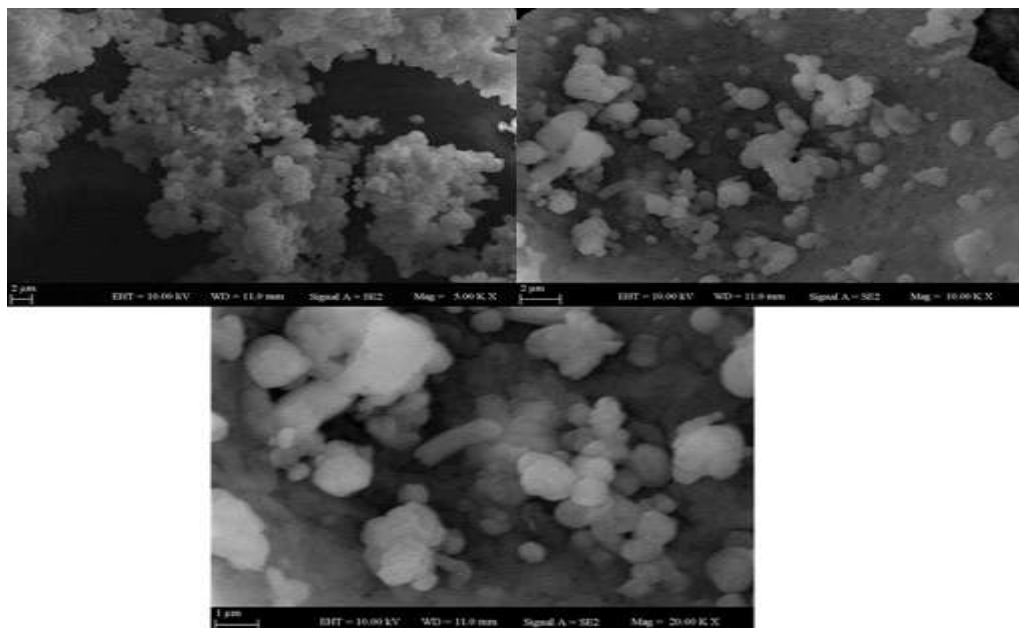


Figure 3.17: SEM micrograph of BMM after calcination.

The SEM micrographs of BMM after drugs loading are shown in Figure 3.18 and Figure 3.19.

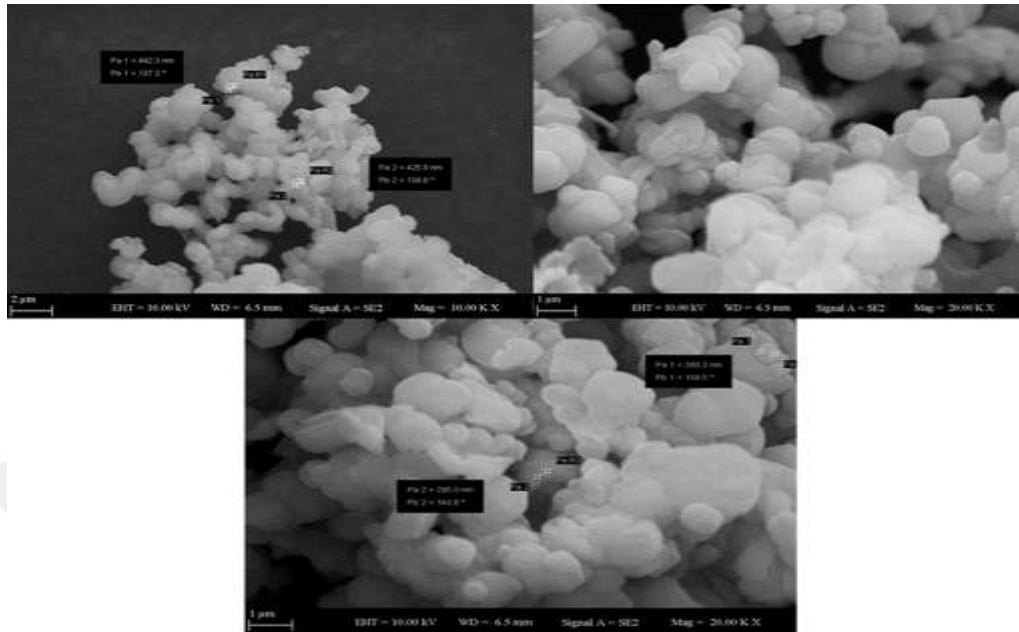


Figure 3.18: SEM micrograph of BMM with 5-Fluorouracil.

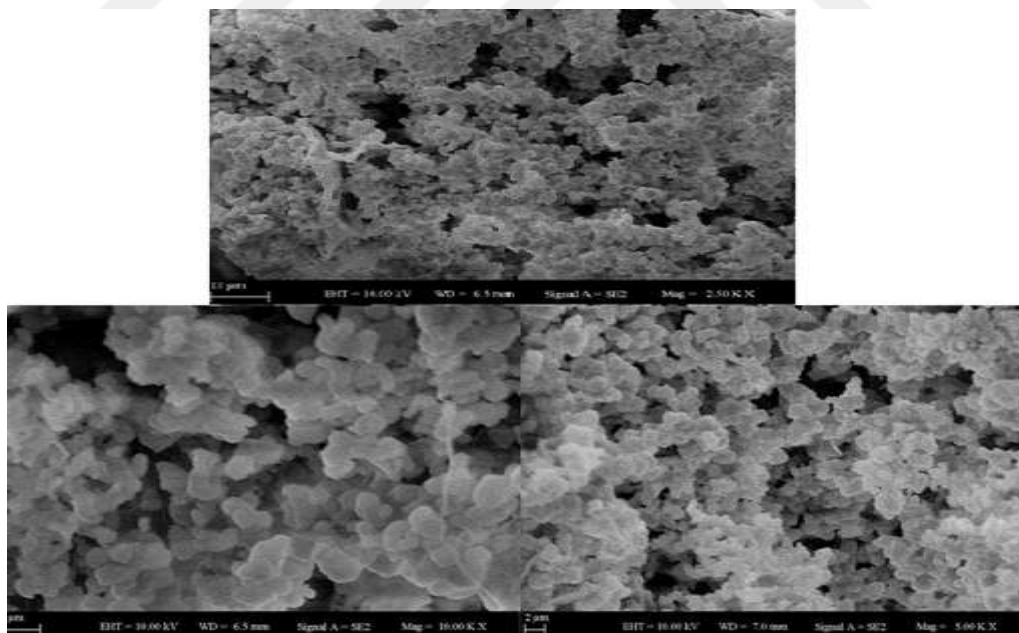


Figure 3.19: SEM micrograph of BMM with ciprofloxacin.

3.2.2. SEM micrograph of TWN 60

SEM results of TWN60 before and after calcination are seen in Figures 3.20 and 3.21.

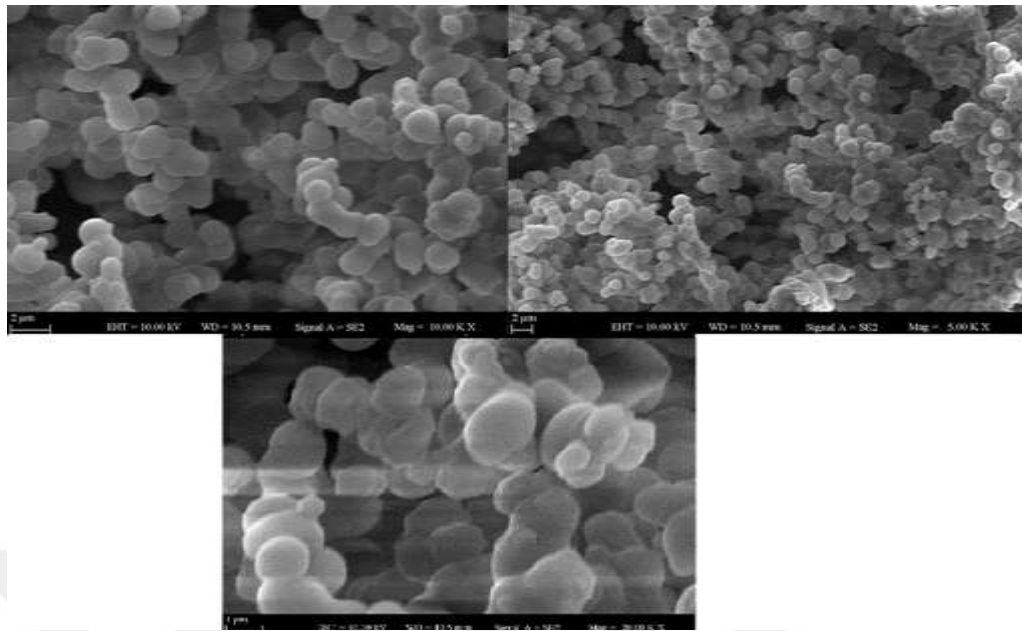


Figure 3.20: SEM micrograph of TWN 60 before calcination.

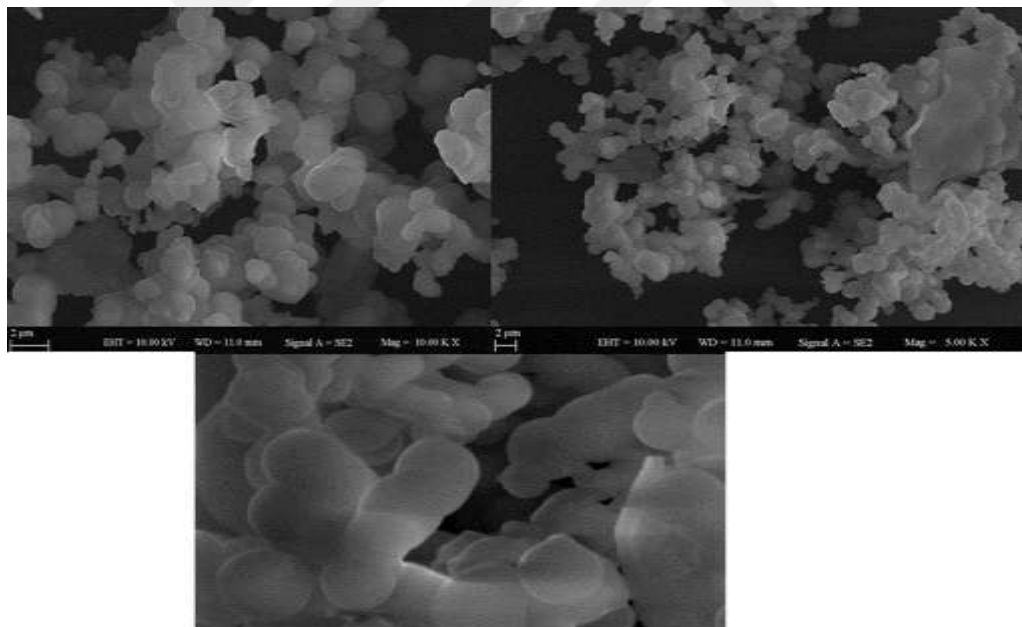


Figure 3.21: SEM micrograph of TWN 60 after calcination.

SEM micrographs of TWN60 loaded with drugs, 5-Fluorouracil and Ciprofloxacin are seen in Figures 3.22 and 3.23, respectively.

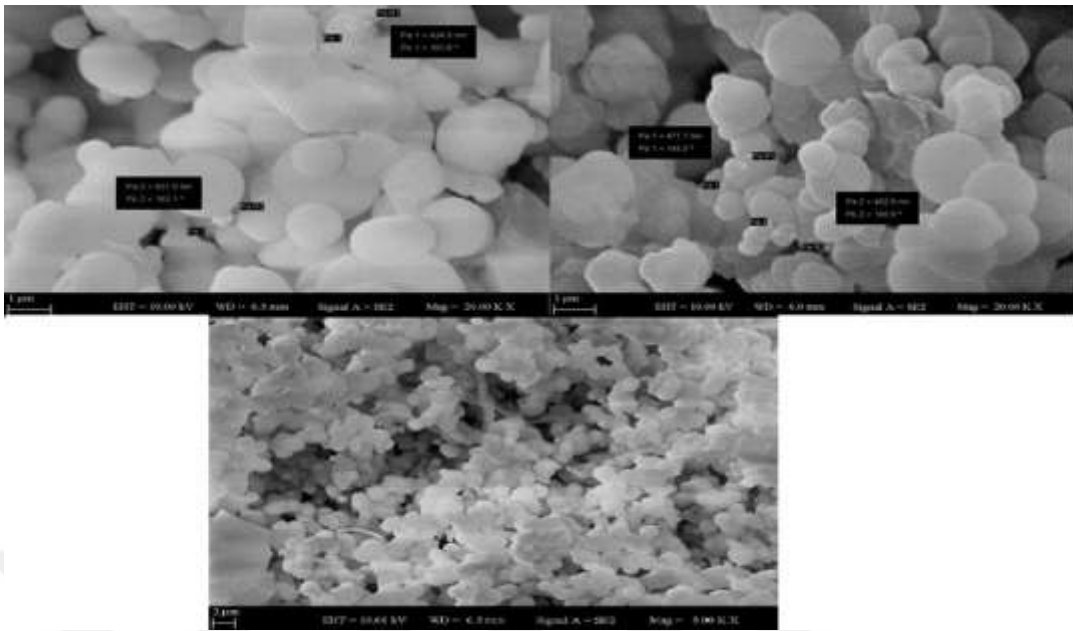


Figure 3.22: SEM micrograph of TWN 60 with 5-Fluorouracil.

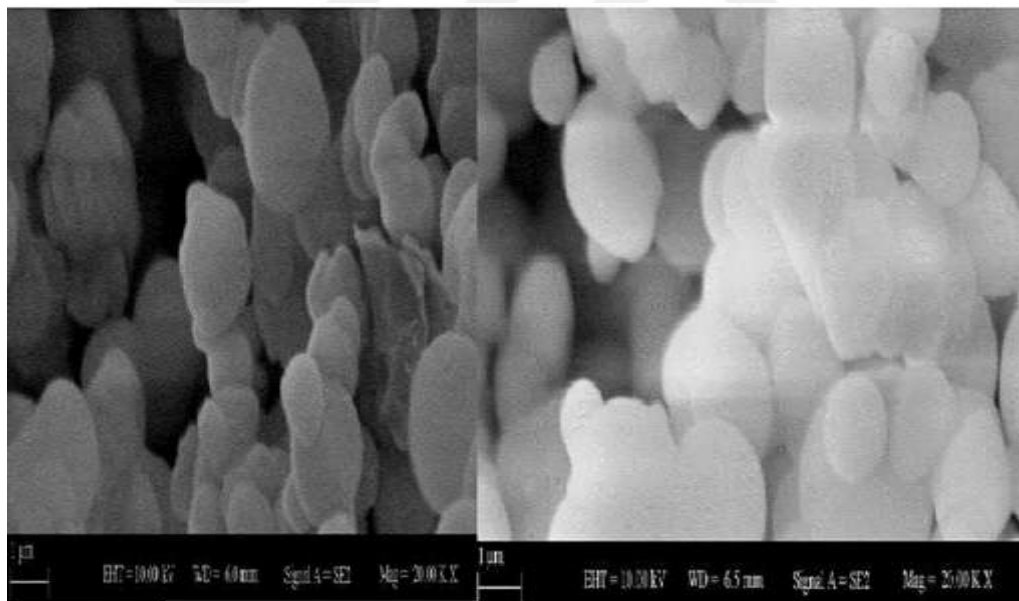


Figure 3.23: SEM micrograph of TWN60 with Ciprofloxacin.

3.2.3. SEM micrograph of TWN 80

SEM micrographs of TWN80 before and after calcination are seen in Figures 3.24 and 3.25.

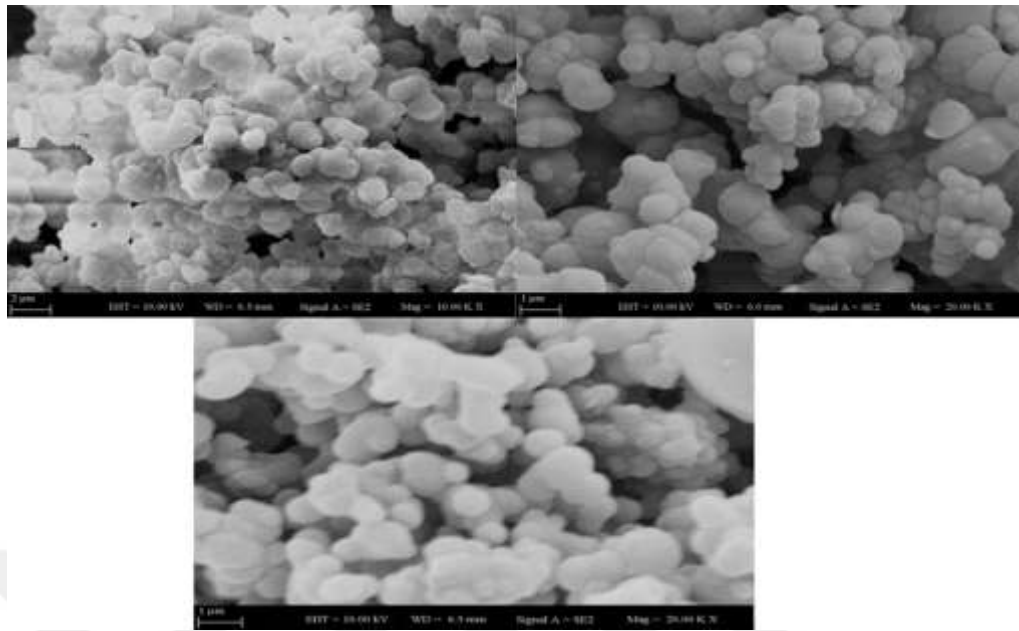


Figure 3.24: SEM micrograph of TWN80 before calcination.

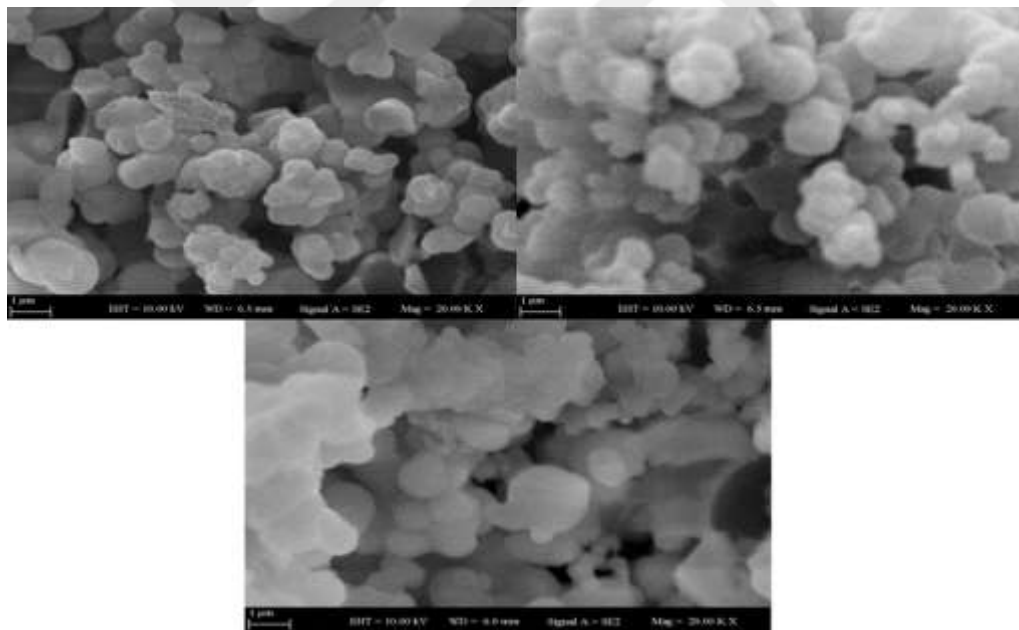


Figure 3.25: SEM micrograph of TWN80 after calcination.

SEM results of TWN80 loaded with drugs, 5-Fluorouracil and Ciprofloxacin are seen in Figures 3.26 and 3.27, respectively.

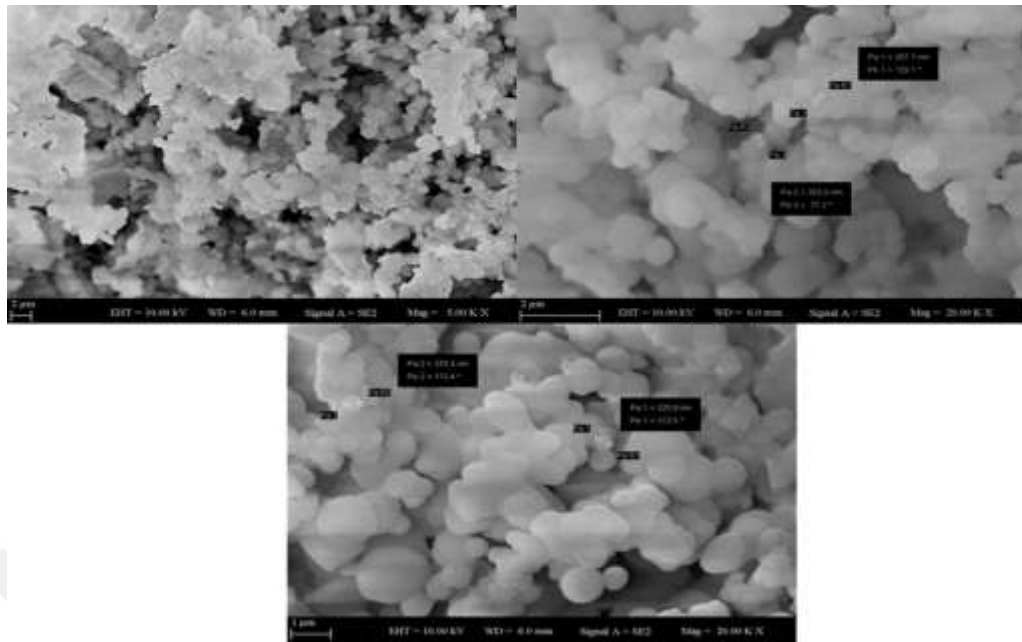


Figure 3.26: SEM micrograph of TWN 80 with 5-Fluorouracil.

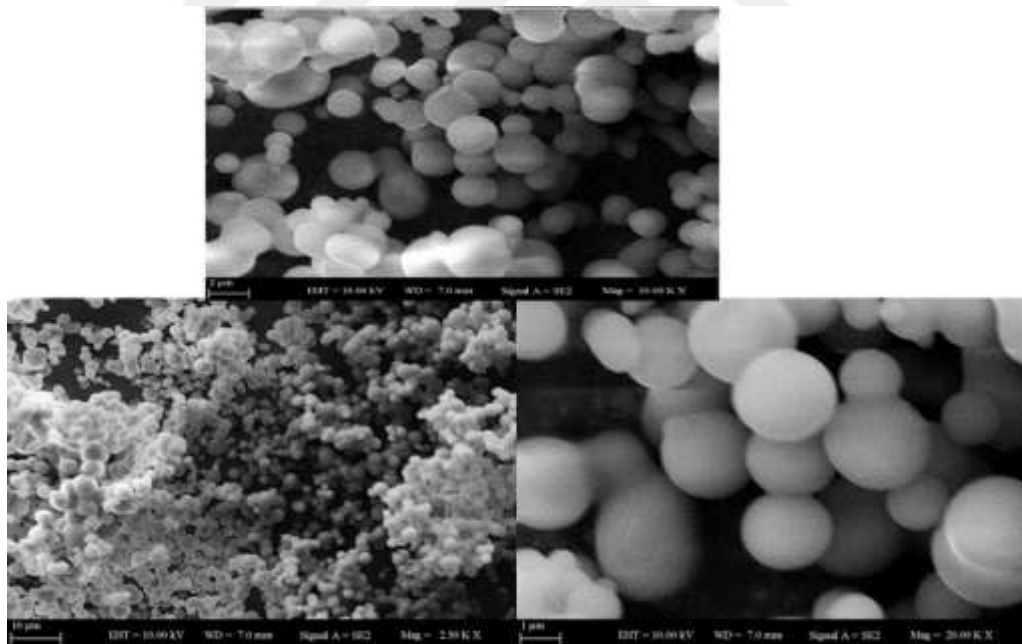
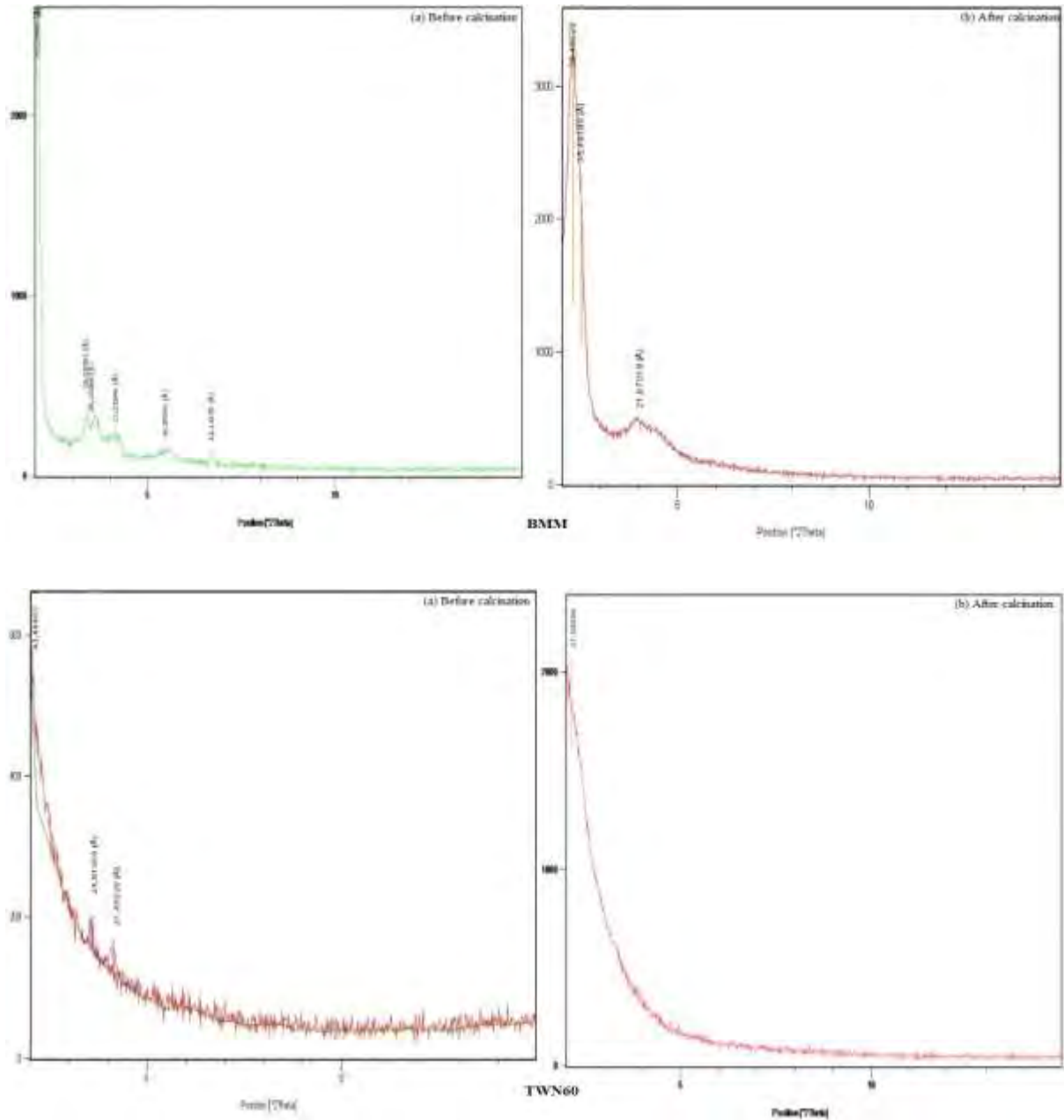


Figure 3.27: SEM micrograph of TWN80 with Ciprofloxacin.

3.3.XRD AND BET STUDIES:

3.3.1. XRD studies of BMM, TWN60, TWN80

Figure 3.28 shows XRD diffractograms of pre-calcinated, post-calcinated, BMM, TWN60, TWN80 samples, respectively.



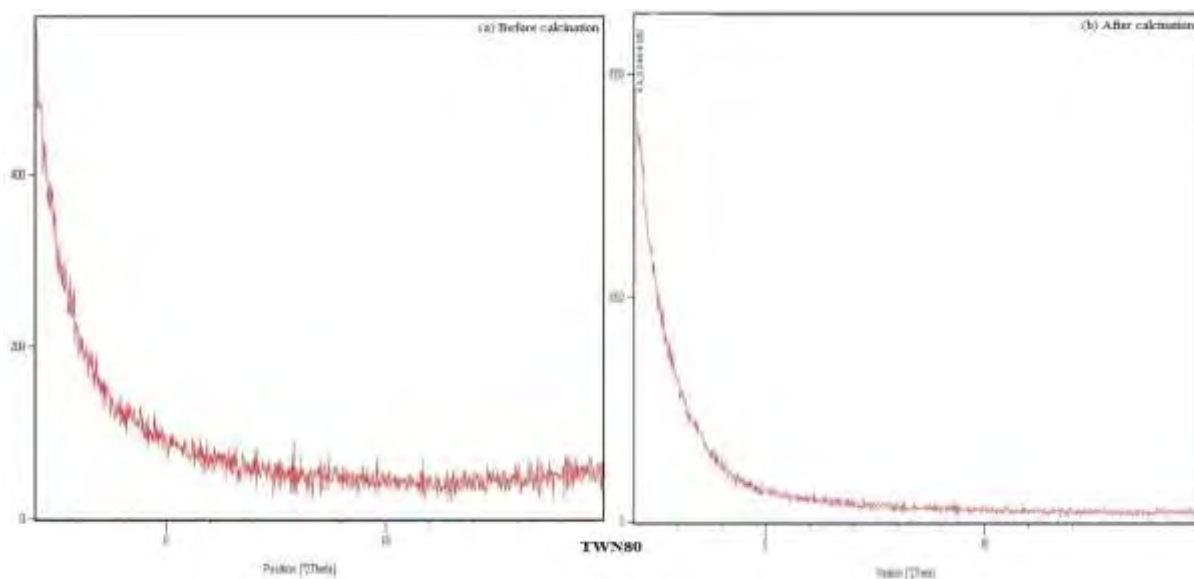


Figure 3.28: XRD-patterns of BMM, TWN60, TWN80 (a) before calcination (b) after calcination.

3.3.2. BET studies:

The TWN60 and BMM mesoporous materials before and after calcination were examined by BET surface area evaluation. The BET surface area of the samples after calcination process are shown in Table 3.1. TWN60 and TWN80 after calcination showed similar porous structure and surface area.

Table 3.1: BET data of prepared samples after calcination process.

samples	Surface area (m ² /g)	Pore volume (cm ³ /g)	Pore diameter (nm)
BMM-after	995.748	0.341	3.129
TWN60-after	666.796	0.711	3.646

3.4. WEIGHT LOSS CALCULATION OF THE SAMPLES

The samples were weighed before and after the calcination process to evaluate the weight loss of the samples by using the following equation:

$$\text{weight loss \%} = \frac{W_{t1} - W_{t2}}{W_{t1}} * 100 \quad (3-1)$$

Where, W_{t1} and W_{t2} are the weight of the samples before and after calcination process, respectively.

By substitution with the BMM experimental data in this equation

$$\text{weight Lost \%} = \frac{2.02-0.82}{2.02} * 100 = 59.4\%$$

The weight loss was found to be 59.4 %

By applying this equation on the data obtained from TWN 60 calcination process.

$$\text{weight Loss \%} = \frac{3.06-1.45}{3.06} * 100 = 52.6\%$$

The weight loss was found to be 52.6 %

And by applying this equation on TWN80

$$\text{weight Loss \%} = \frac{6.10-1.54}{6.10} * 100 = 74.8\%$$

The weight loss was found to be 74.8 %

3.5.DRUG RELEASE AND DELIVERY STUDIES

Drug delivery and release profiles were followed using UV-spectrometer by measuring the absorbance of the solutions at the max-absorbance values of the drugs.

3.5.1. Standard Curve of 5-Fluorouracil

Before studying the drug delivery and release experiments, the standard curves of the drugs were obtained by using different drug concentrations. For this purpose, the stock solution of 5-Fluorouracil (60 ppm) was prepared and diluted to different concentrations of this drug. The absorbance of 5-Fluorouracil solutions was measured at the wavelength 266nm by UV-Visible spectrophotometer. (Figure 3.29)

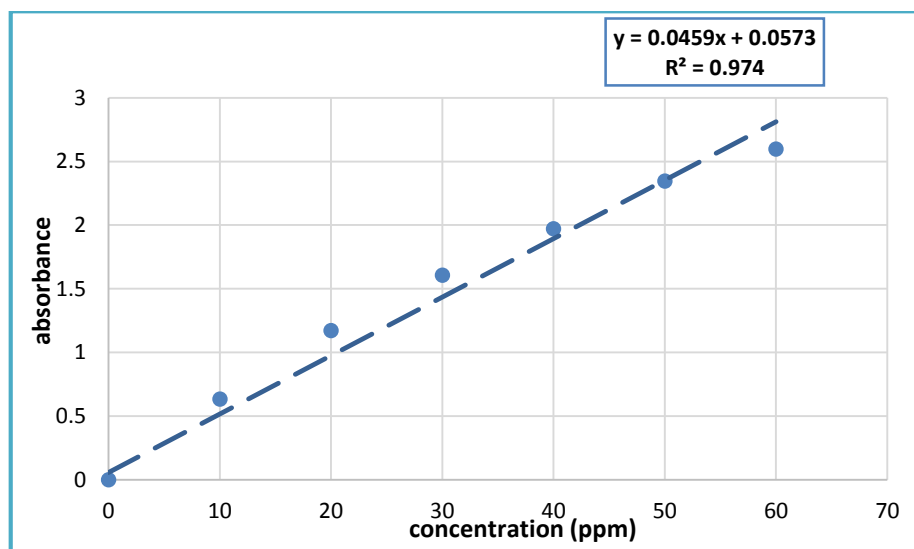


Figure 3.29: Standard Curve of 5-Fluorouracil.

3.5.2. Delivery and release of 5-Fluorouracil loaded to BMM

The BMM sample was kept in 50ml, 20ppm 5-Fluorouracil drug solution until the drug loading process reached an equilibrium. The equilibrium was reached in 150min. Release of 5-Fluorouracil took place in different media and the graph was shown in Figure 3.30.

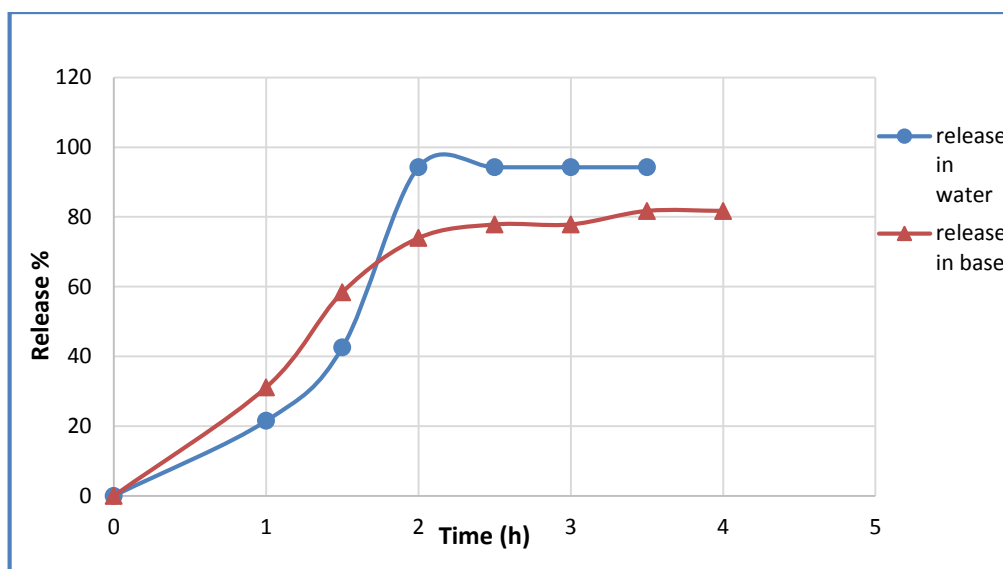


Figure 3.30: Release of 5-Fluorouracil loaded to BMM.

Release of the drug was calculated according to first order, zero order, Korsmeyer-Peppas and Higuchi models. The kinetic constants of the release of drugs were calculated and the results were presented in Table 3.1.

Table 3.2: Release constants of 5-Fluorouracil loaded to BMM in different media.

Kinetics→	Zero order		First order		Higuchi model		Korsmeyer-Peppas model		
	K_0 (mol.l ⁻¹ .h ⁻¹)	R^2	K_1 (h ⁻¹)	R^2	K_H (h ^{1/2})	R^2	K_m (h ⁿ)	n	R^2
*BMM _w	0.149	0.979	0.587	0.899	0.316	0.982	0.424	1.166	0.969
*BMM _b	0.175	0.873	0.369	0.956	0.327	0.978	0.856	0.228	0.974

*BMM_w and *BMM_b are the release of drug loaded BMM in aqueous medium and basic medium, respectively.

3.5.3. Delivery and release of 5-Fluorouracil loaded to TWN60

TWN60 sample was kept in 50 ml, 20ppm 5-Fluorouracil drug solution. The loading time was found to reach equilibrium in 120 min. Release of 5-fluorouracil took place in different media and the graph was demonstrated in Figure 3.31. The drug release was examined and the release kinetic constants have been calculated. The results are presented in table 3.2.

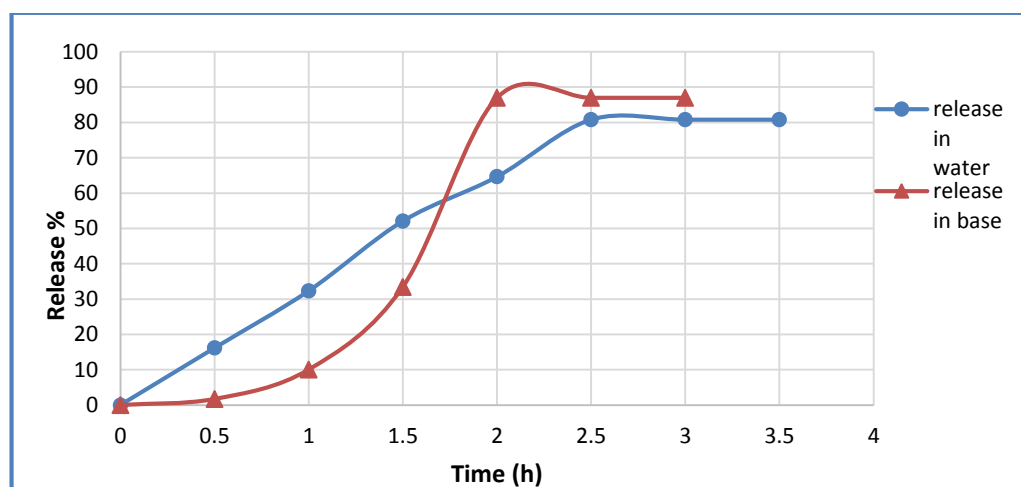


Figure 3.31: Release of 5-Fluorouracil loaded to TWN 60.

Table 3.3: Release constants of 5-Fluorouracil loaded to TWN 60 in different media.

Kinetics→	Zero order		First order		Higuchi model		Korsmeyer-Peppas model		
	K_0 (mol.l ⁻¹ .h ⁻¹)	R^2	K_1 (h ⁻¹)	R^2	K_H (h ^{1/2})	R^2	K_m (h ⁿ)	n	R^2
TWN60 _w	0.395	0.998	0.237	0.988	0.617	0.918	0.758	0.273	0.979
TWN60 _b	2.693	0.880	1.375	0.992	1.576	0.753	0.956	0.746	0.937

*TWN60_w and TWN60_b are the release of drug loaded TWN60 in aqueous medium and in basic medium, respectively.

3.5.4. Delivery and release of 5-Fluorouracil loaded to TWN80

TWN80 sample was kept in 50 ml, 20ppm 5-Fluorouracil drug solution. The loading time was found to reach equilibrium in 60 min. Release of 5-Fluorouracil took place in different media and the graph was demonstrated in Figure 3.32. The drug release was examined and the release kinetic constants were calculated. The results are presented in table 3.3.

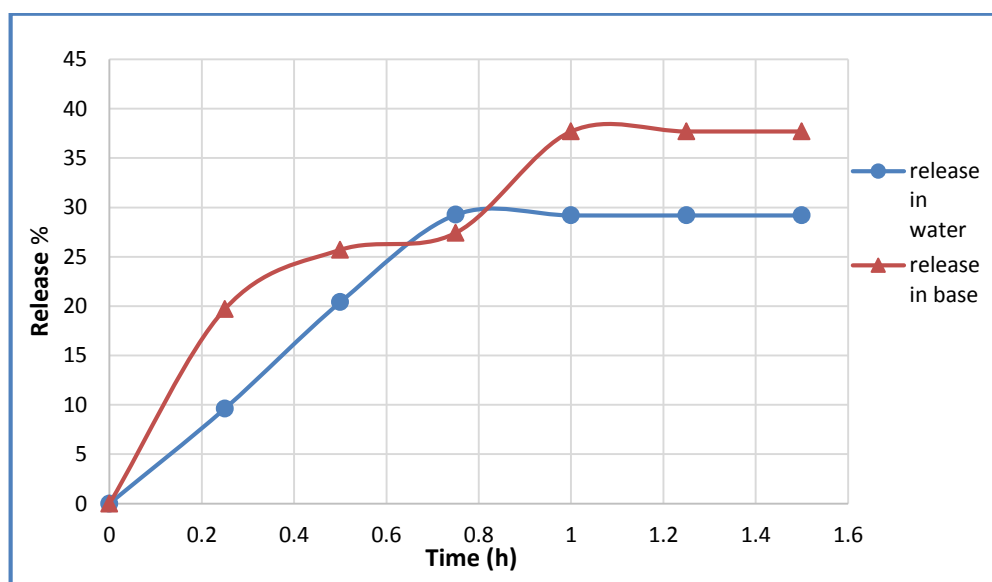


Figure 3.32: Release of 5-Fluorouracil loaded to TWN 80.

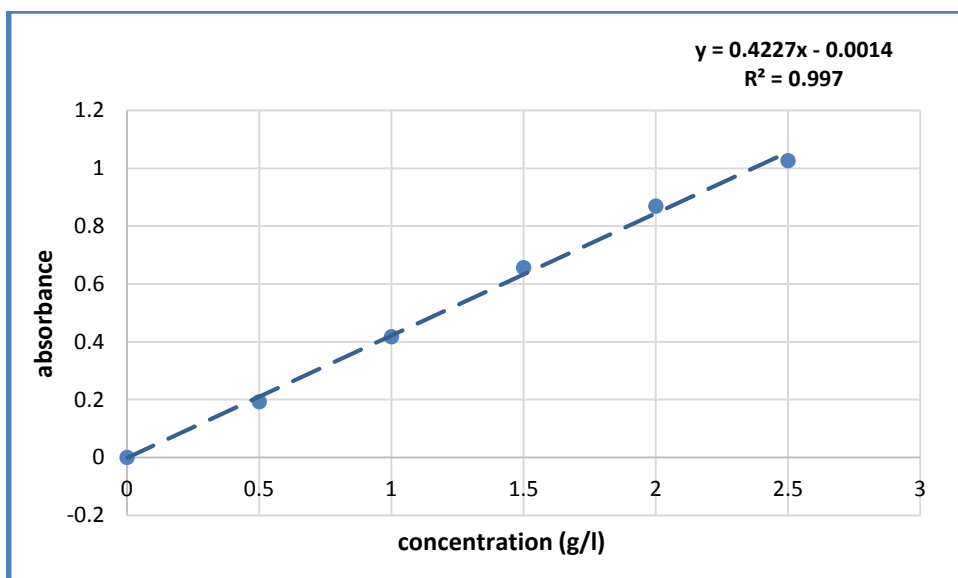
Table 3.4: Release constants of 5-Fluorouracil loaded to TWN 80 in different media.

Kinetics→	Zero order		First order		Higuchi model		Korsmeyer-Peppas model		
	K ₀ (mol.l ⁻¹ .h ⁻¹)	R ²	K ₁ (h ⁻¹)	R ²	K _H (h ^{1/2})	R ²	K _m (h ⁿ)	n	R ²
*TWN80 _w	1.699	0.996	0.346	0.91	1.842	0.927	1.039	0.148	0.995
*TWN80 _b	3.151	0.851	0.669	0.896	0.501	0.652	0.081	0.517	0.923

*TWN80_w and *TWN80_b are the release of drug loaded TWN80 in aqueous medium and in basic medium, respectively.

3.5.5. Standard Curve of Ciprofloxacin

The stock solution of Ciprofloxacin was prepared (2.5g/l) and diluted to different concentrations. The absorbance of Ciprofloxacin solutions was measured at the wavelength 390 nm by UV-Visible spectrophotometer. (Figure 3.33)

**Figure 3.33:** Standard Curve of Ciprofloxacin.

3.5.6. Delivery and release of Ciprofloxacin loaded to BMM

The BMM sample was kept in 50ml, 1.5g/l Ciprofloxacin drug solution until the drug loading process reach an equilibrium. The equilibrium was reached in 120 min. Release of Ciprofloxacin loaded to BMM took place in different media and the graph was demonstrated in Figure 3.34. Release of the drug was calculated using first order, zero order, Korsmeyer-Peppas and Higuchi models. The kinetic constants of the release of drugs have been calculated and presented in table 3.4.

Table 3.5: Release constants of Ciprofloxacin Loaded to BMM in different media.

Kinetics→	Zero order		First order		Higuchi model		Korsmeyer-Peppas model		
	K ₀ (mol.l ⁻¹ .h ⁻¹)	R ²	K ₁ (h ⁻¹)	R ²	K _H (h ^{1/2})	R ²	K _m (h ⁿ)	n	R ²
BMM_w	0.093	0.963	0.198	0.977	0.172	0.833	0.663	0.292	0.863
BMM_a	0.077	0.948	0.147	0.933	0.164	0.927	0.734	0.248	0.942

*BMM_a is the release of drug loaded BMM in acidic medium.

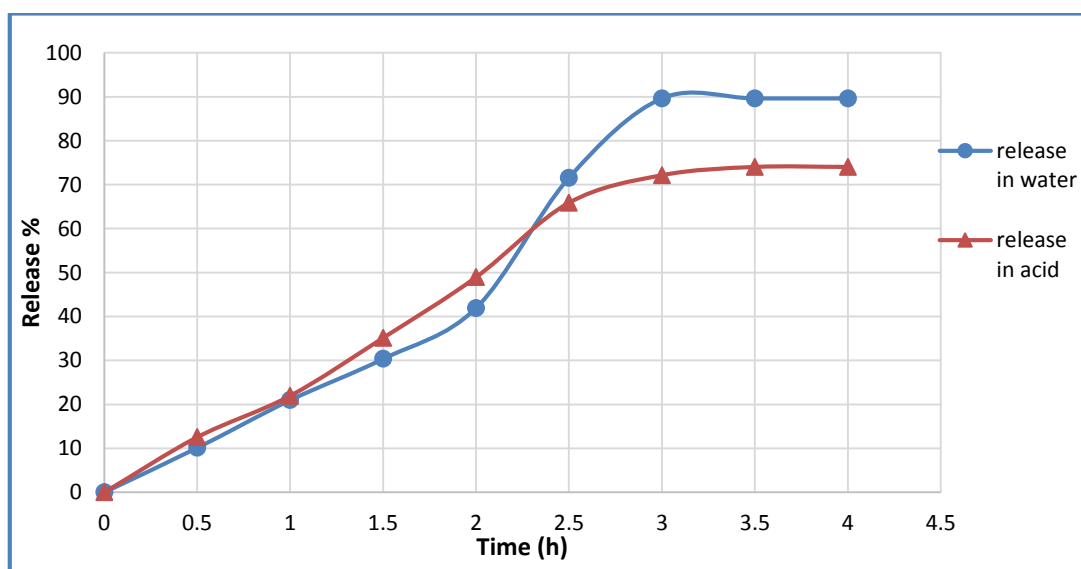


Figure 3.34: Release of Ciprofloxacin Loaded to BMM.

3.5.7. Delivery and release of Ciprofloxacin loaded to TWN60

TWN60 sample was kept in 50 ml, 1.5g/l Ciprofloxacin drug solution. The loading time was found to reach equilibrium in 150 min. Release of Ciprofloxacin loaded to TWN 60 took place in different media and the graph was demonstrated in Figure 3.35. The drug release was calculated and the drugs release kinetic constants have been calculated (table 3.5).

Table 3.6: Release constants of Ciprofloxacin Loaded to TWN 60 in different media.

Kinetics→	Zero order		First order		Higuchi model		Korsmeyer-Peppas model		
	K_0 (mol.l ⁻¹ .h ⁻¹)	R^2	K_1 (h ⁻¹)	R^2	K_H (h ^{1/2})	R^2	K_m (h ⁿ)	n	R^2
TWN60 _w	0.080	0.967	0.119	0.981	0.134	0.819	0.780	0.138	0.957
TWN60 _a	0.081	0.965	0.176	0.963	0.158	0.933	0.760	0.231	0.982

*TWN60_a is the release of drug loaded TWN60 in acidic medium.

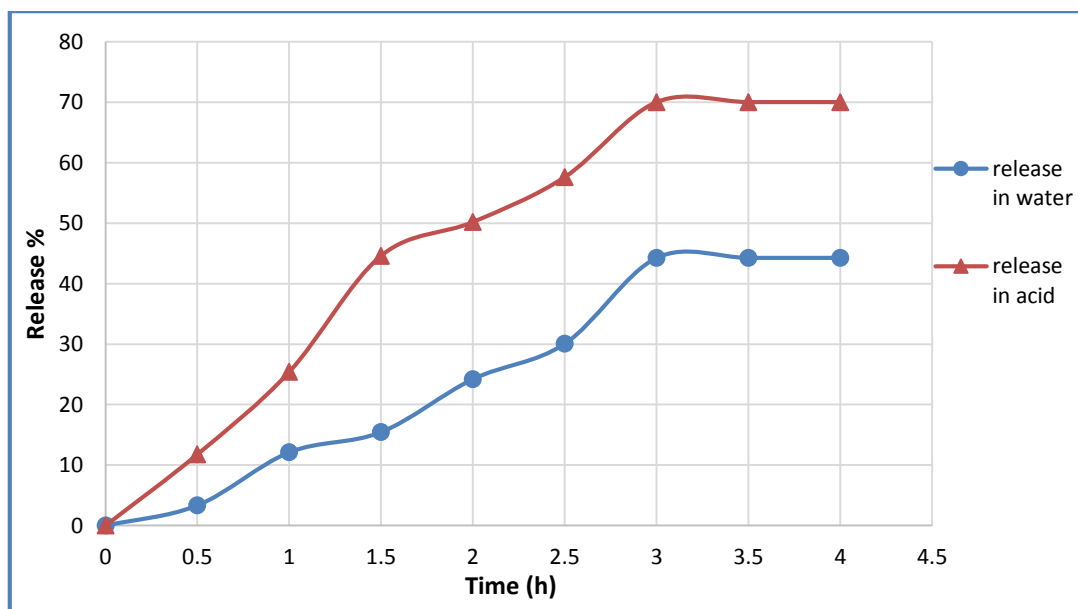


Figure 3.35: Release of Ciprofloxacin loaded to TWN 60.

3.5.8. Delivery and release of Ciprofloxacin Loaded to TWN 80

TWN80 sample was kept in 50 ml, 1.5g/l Ciprofloxacin drug solution. The loading time was found to reach equilibrium in 180 min. Release of Ciprofloxacin took place in different media and the graph was demonstrated in Figure 3.36. The drug release was calculated and the drugs release kinetic constants have been calculated (table 3.6).

Table 3.7: Release constants of Ciprofloxacin loaded to TWN 80 in different media.

Kinetics→	Zero order		First order		Higuchi model		Korsmeyer-Peppas model		
	K_0 (mol.l ⁻¹ .h ⁻¹)	R ²	K_1 (h ⁻¹)	R ²	K_H (h ^{1/2})	R ²	K_m (h ⁿ)	n	R ²
TWN80 _w	0.124	0.954	0.225	0.949	0.219	0.894	0.735	0.284	0.878
TWN80 _a	0.096	0.940	0.209	0.956	0.193	0.949	0.752	0.262	0.966

*TWN80a is the release of drug loaded TWN80 in acidic medium.

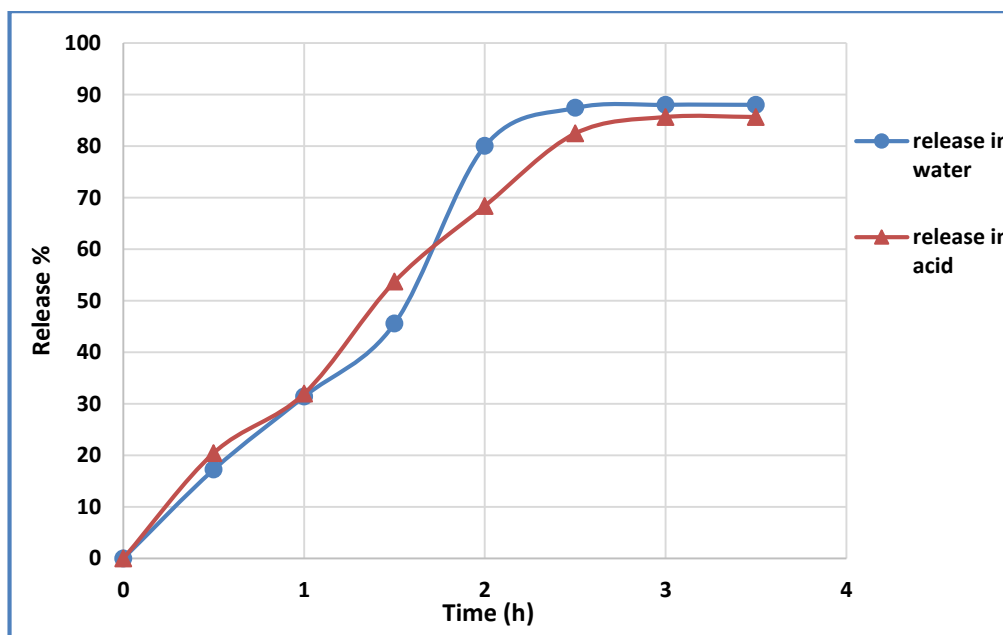


Figure 3.36: Release of Ciprofloxacin loaded to TWN 80.

4. DISCUSSION

In this study, three different mesoporous drug carriers were prepared to examine the loading and release profiles of two different various drug active substances. The prepared drug carrier were abbreviated as; BMM, TWN60 and TWN80. 5-Fluorouracil and Ciprofloxacin were used as model drugs. Structural and morphological characterizations of these samples were investigated by using FTIR, SEM and XRD.

The FTIR spectra of pure substances TEOS, 5-Fluorouracil and Ciprofloxacin were first analyzed to be compare afterwards with the structure of the prepared and drug loaded samples. Figure 3.1 shows FTIR spectrum of TEOS, while Figures 3.2 and 3.3 represent FTIR spectra of drugs containing 5-Fluorouracil and Ciprofloxacin, respectively. In Figure 3.2 the peak observed at 3065.30cm^{-1} identifies with the N-H bond, 2930.06cm^{-1} indicates C-H bond stretching vibrations and 1644.77cm^{-1} corresponds to carbonyl-group stretching vibrations [73]. The peaks at 1266.4cm^{-1} belong to the C-F bond stretching vibrations and at peak at 1622.11cm^{-1} relates to the -COOH group stretching vibrations of phenyl rings seen in Figure 3.3. The peaks observed at 2926.71cm^{-1} and 3084.83cm^{-1} are characteristic bands for the C-H stretching vibrations of the phenyl ring of Ciprofloxacin.

The FTIR spectra of all of the prepared samples before and after calcination were comparatively analyzed. As such, it was possible to see the changes in the samples' characteristic absorption bands and investigate if the loaded drug could still maintain its efficiency even after being loaded into the sample.

Before calcination, FT-IR studies were performed for BMM and the results are shown in Figure 3.4. It showed a medium peak at wavenumber 2921.71cm^{-1} and a small peak at wavenumber 2852.04cm^{-1} which are assigned to aliphatic C-H bond. Another peak at wavenumber 1478.85cm^{-1} can be ascribed to C-N bond. A broad and long peak at 1026.86cm^{-1} and the small peak at wavenumber 781.40cm^{-1} relate to (symmetric-asymmetric) Si-O-Si bonds. The characteristic peaks observed at 1026.86cm^{-1} and 781.40cm^{-1} in the spectrum of BMM before calcination (in figure 3.4) shifted to a broad peak at wavenumber 1046.26cm^{-1} and a narrow peak at wavenumber 803.59cm^{-1} After the calcination of BMM, as shown in Figure 3.5 Also, all other peaks become weaker and wider which were observed at 2921.71cm^{-1} and 2852.04cm^{-1} before calcination. These peaks are

overlapped forming a wide small peak. These results showed that the calcination process affects the structure of the samples.

FTIR spectrum of the 5-Fluorouracil-loaded on calcinated BMM samples shows the broadening and overlapping of the 3065.30 cm^{-1} and 2930.06 cm^{-1} peaks of N-H and C-H bond vibrations that were separate and distinguishable before loading in 5-Fluorouracil spectrum (Figure 3.2). Similarly, peaks observed at 1449.19 cm^{-1} and 1503.89 cm^{-1} on the FTIR spectrum of 5-Fluorouracil can be seen to overlap at 1054.10 cm^{-1} in Figure 3.6. On the other hand, the peak seen at 1644.77 cm^{-1} shifted to 1636.81 cm^{-1} while having significantly shrunk in size. Also, the peak appearing at 802.84 cm^{-1} before loading can be seen to shift slightly to the range of 791.98 cm^{-1} in 5-Fluorouracil-loaded on calcinated BMM samples (Figure 3.6). Similar results were obtained with Ciprofloxacin-loaded BMM samples. The narrow peaks between 1609.04 and 1023.57 cm^{-1} on Ciprofloxacin FTIR spectrum can be seen to overlap at 1053.64 cm^{-1} as a narrow peak having a shoulder (Figure 3.7). These results showed that both drugs were adsorbed by the BMM drug carriers.

FT-IR spectrum of TWN60 before calcination (figure 3.8) shows a small peak (at wavenumber 2922.32 cm^{-1}) related to C-H aliphatic bond. The long and large peak observed at wavenumber 1046.32 cm^{-1} related to Si-O-Si bonds. The small two peaks arising at wavenumber 949.69 cm^{-1} and 796.41 cm^{-1} are ascribed to =C-H alkene group. FT-IR spectrum of TWN 60 after calcination showed a smooth structure and the peaks observed at 1511.87 cm^{-1} and 1456.24 cm^{-1} before calcination overlapped at 1639.36 cm^{-1} after calcination. All other peaks shifted slightly to higher wavenumbers. These results show that the calcination process helps the samples to obtain a more ordered structures (Figure 3.9). The FTIR spectrum after loading 5-Fluorouracil on calcinated TWN60 showed that drug active ingredient was held by drug carrier (Figure 3.10). Similar results were seen on the FTIR spectrum of calcinated TWN60-loaded Ciprofloxacin. (Figure 3.11). Comparing TWN80 before and after calcination shows that after calcination, the sample obtains a more ordered structure. Pre-calcination peak at 3299.00 cm^{-1} and 2874.13 cm^{-1} overlap at a broad peak at 3354.47 cm^{-1} after calcination. Similar results of FTIR spectrum of TWN80 (Figure 3.12, and Figure 3.13) were observed with the spectrum of TWN60. Both drugs did not react with the prepared samples in this work. The drugs were physically absorbed by these carriers as shown in FTIR Figures as mentioned within the literature [70] [74].

The morphological analysis of the prepared samples was done with the aid of a Scanning Electron Microscope (SEM) and their micrographs were examined in order to assess their morphological features. The micrographs were obtained before and after the calcination processes.

After the calcination process, SEM micrographs of 5-Fluorouracil and Ciprofloxacin-loaded samples were also taken. The interaction between the scaffold and the drug was assessed by comparing the morphological features of the scaffold, before and after drug loading.

For the BMM sample, pre-calcination SEM micrographs show a more dense and packed structure whereas post-calcination micrographs appear to have a tighter and more porous structure (Figures 3.16 and 3.17).

SEM micrographs of the scaffold after being loaded with 5-Fluorouracil show the attachment and aggregation of this drug onto the porous structure whereas Ciprofloxacin appears to have homogeneously distributed along the scaffold surface (Figures 3.18 and 3.19).

Comparison of the SEM micrographs of the prepared TWN60 samples pre- and post-calcination shows that the homogeneous and dense structure that is present before calcination takes on a smoother and more porous structure after being calcinated (Figure 3.20-Figure 3.21). With a homogeneous distribution that can be observed for both of the model drugs, no significant difference in their morphological structure can be seen between the drug-loaded samples (Figure 3.22-Figure 3.23). Comparison of the SEM micrographs of the prepared TWN80 carriers before and after calcination indicates that the continuous and dense structure that is present before calcination takes on a more porous structure after being calcinated (Figure 3.24-Figure 3.25). The homogeneous distribution was observed for both of the drugs seen in figure 3.26 for 5-fluorouracil. Ciprofloxacin loaded on TWN80 sample showed a more ordered structure (Figure 3.27).

XRD patterns of the BMM samples prepared before (a) and after (b) calcination are seen in Figure 3.28. The XRD profile of pre-calcinated BMM sample showed characteristic peaks at 2θ between 0° and 5° . Both BMM samples represent one strong peak at 2θ between 0° and 2° with d spacing of 42.64Å and 38.67Å, respectively. The other small peaks observed

between 2° and 5° were overlapped and slightly decreased of d values after calcination, as expected. The XRD diffractogram of BMM with a narrow high peak confirmed the existence of SiO₂ nanoparticles in BMM matrix. These patterns with low angles indicate the presence of arrays with organized pores of MSNs. Calcination of BMM at 550^oC for 5h shows better XRD patterns as in figure 3.28 (b). After calcination, the XRD pattern showed that the smooth structure and the intensity of the peaks decreased. A similar pattern was observed after loading the model drugs.

By comparing XRD results of TWN60 before and after calcination it can be observed that there are not much differences between the patterns. The first strong peaks of the samples are seen at 2θ between 0° and 1° with d spacing approximately 42^oA. The other small peaks observed between 2° and 5° were overlapped and a slight decrease of d values, as expected.

XRD patterns of the sample TWN80 did not significant change before and after calcination process represented in Figure 3.28 (a) and (b). XRD results show well-ordered mesoporous structures of all samples after calcination as reported by Zhao and co-workers [56].

Pore size distribution of the samples were taken by BET analysis. Because of the pore size of the samples observed between 2 and 10 nm, all samples are shown the mesoporous structure (Table3.1).

It can be observed that the mesoporous samples with narrow pore size distribution, high porosity and high surface area were successfully synthesized in this work. These pores samples are very effective for the drug delivery and release experiments for the model drugs 5-Fluorouracil and Ciprofloxacin used in this study.

During the loading process, the absorbance of the drugs in solutions was measured between predetermined intervals of time. The absorbance of the drug solutions decreases with time until reaching a steady state. Concentration of the drug solutions was estimated by using the standard curves of the drugs. The time it took for loading to reach an equilibrium for 5-Fluorouracil and Ciprofloxacin on BMM was observed 150 min and 120 min, respectively. The drug release until steady state from TWN60 for the drugs 5-Fluorouracil and Ciprofloxacin was found to be 120 and 150 min respectively. 5-Fluorouracil was loaded on TWN80 with high uptake percentage and in a short time compared to the loading of Ciprofloxacin on the same carrier. The adsorption of Ciprofloxacin on BMM showed better

results than that of 5-Fluorouracil. Small amount of 5-Fluorouracil was taken by BMM. On the other hand, Ciprofloxacin loaded on BMM was three times higher than that of 5-Fluorouracil.

The release profile of the drugs was examined in distilled water and two buffer solutions with pH= 2 and pH= 7.6. Almost 95% of 5-Fluorouracil released from BMM in distilled water while 81% released in basic media. The release of 5-Fluorouracil in acidic medium was not favorable. For both releasing media, the time necessary to reach equilibrium from loaded BMM was almost the same (2 hours) (Figure 3.30). 81% of 5-Fluorouracil released from TWN60 in distilled water while 88% released in basic medium (Figure 3.31). The release time to reach equilibrium is 2h (in the base) and 2.5h (in distilled water). For 5-Fluorouracil, release time from loaded TWN80 is shorter than the other drug carriers. It reaches on equilibrium in approximately 1h. (Figure 3.32)

When it comes to the Ciprofloxacin release from these carriers the efficient results were obtained in distilled water and acidic medium. Ciprofloxacin released from BMM in Water (90%) is higher than in pH= 2 solvent (75%). Reaching equilibrium takes three hours for both media as shown in Figure 3.34. Comparing the release percentage of Ciprofloxacin for TWN60 and TWN80 it can be seen that higher value were obtained for the TWN80 carrier, both in acidic medium and in distilled water. Reaching to the equilibrium of the release profile is longer for TWN60 (3 hours) than that of TWN80 (2.5 hours). (Figures 3.35 and 3.36). Similar results were reported in the literature for other types of MNPs [55].

Various models were applied to examine the drug release kinetics from drug carriers prepared in this study. The kinetic coefficients and R^2 values obtained from the kinetic calculations of these models were estimated and the results were given in tables 3.1 - 3.6.

The release of 5-Fluorouracil drug active substance loaded on BMM was found to be zero order kinetic ($R^2 = 0.979$) and fitting the Higuchi model ($R^2 = 0.982$) in distilled water. Zero order kinetic shows that the release amount of the drug active ingredient remained constant over time. Besides, the suitability of the Higuchi model shows that release of 5Fluorouracil is assumed to occur by diffusion. The release kinetics of the 5-Fluorouracil drug active substance in buffer solution (pH = 7.6) were also examined. It is considered that the release

is fits the Higuchi model ($R^2 = 0.978$) and therefore the release of 5-Fluorouracil is assumed to occur by diffusion.

Similar studies about Ciprofloxacin loading on BMM showed that the release of drug in distilled water fits the 1st order kinetics. This results indicates that the amount of drug released decreases with time. The release of ciprofloxacin drug active substance at pH = 2 buffer solution corresponds to a zero order kinetics. According to this result, the release of the drug-active substance remains constant over time.

The release of 5-Fluorouracil drug active substance from TWN60 in water was found to be zero order kinetic ($R^2 = 0.998$) and fitting Korsmeyer-Peppas model ($R^2 = 0.979$) in distilled water. Zero order kinetic shows that the release amount of the drug active ingredient remained constant over time. The “n values” calculated according to the Korsmeyer-Peppas model were estimated between 0.2 and 1.0 ($n = 0.273$ for the release in water and $n = 0.746$ for the release in buffer solution) which corresponds to the type of diffusion that is effective in the swelling and loosening of the drug carrier material prepared in this work, this type of diffusion is called the abnormal transport of the drug release.

Ciprofloxacin loading on TWN60 showed that the release of drug in distilled water fits the 1st order kinetics. This result indicates that the amount of drug released decreases with time. The release of ciprofloxacin drug active substance at pH = 2 buffer solution corresponds to zero-order and fits the Korsmeyer-Peppas model. According to this result, the release of the drug-active substance remains constant over time.

Similar results were observed for the TWN80 drug carrier. The release of 5-Fluorouracil drug active substance from TWN80 in water was found to be zero order kinetic ($R^2 = 0.91$) and fitting the Korsmeyer-Peppas model ($R^2 = 0.995$) in distilled water. Zero order kinetic shows that the release amount of the drug active ingredient remained constant with time. The “n values” calculated according to the Korsmeyer-Peppas model were also found as $n = 0.148$ for the release in water and $n = 0.517$ for the release in buffer solution.

In this study, it was seen that both drug active substances were physically loaded to the prepared drug carriers without any chemical reactions and the release time and release amounts of the drug active substances from the prepared drug carriers were reasonable when compared to the literature[75][76].

5. CONCLUSION AND RECOMMENDATIONS

In this study three different scaffolds were prepared for the drug delivery systems and the release profiles of drugs were kinetically examined. Two types of drugs, 5-Fluorouracil (anti-cancer drug) and Ciprofloxacin (antibiotic drug) were used as model drugs. During the experiments, three types of mesoporous nanoparticles were prepared, BMM, TWN 60 and TWN 80. Each mesoporous samples was calcinated and then loaded with these drugs. Different surfactants were used to prepare these scaffolds which are CTAB, Tween60, Tween80 and TritonX-100.

The properties of these scaffolds were studied by FT-IR, SEM, XRD, BET and from these characterizations it was found that the surfactants during calcination which loss in weight and the porosity structure clearly observed after calcination. The efficiency of loading and release were examined, and it was observed that the drug was efficiently and physically loaded inside the scaffolds. The release of the drug took place in three different pH media which are aqueous, pH = 2 (similar of stomach acidity) and pH = 7.6 (approximate to intestine pH). All results were measured by using UV-vis spectrophotometry and calculated with kinetics equations which are Zero order, First order, Higuchi model and Korsmeyer-Peppas model.

In this study, FTIR spectra of all of the prepared samples were analyzed before and after calcination as well as before and after drug loading. As a result of these analyses, it was seen that the drug active ingredients that were loaded into the prepared hydrogels were able to bond with the scaffold without any noticeable structural alterations. Also, from these FTIR analyses, since no new characteristic peaks appear on the FTIR spectra of drug-loaded scaffolds, it can be concluded that no chemical reaction takes place between the drug and its carrier. As such, it can be deduced that both drug active ingredients do not lose their efficiency during drug loading and release.

From the release profile of the drugs in different media and from the kinetics calculations, it is found that both drugs released from each scaffold efficiently with reasonable time. It can be concluded that these three scaffolds are good carriers for 5-Fluorouracil and Ciprofloxacin drugs.

REFERENCES

- [1] Vallet-Regí, M., 2006, Ordered mesoporous materials in the context of drug delivery systems and bone tissue engineering, *Chemistry-A European Journal*, 12 (23), 5934-5943.
- [2] Allen, T.M., and Cullis, P.R., 2004, Drug delivery systems: entering the mainstream. *Science*, 303 (5665), 1818-1822.
- [3] Jeong, B., Bae, Y.H., Lee, D.S. and Kim, S.W., 1997, Biodegradable block copolymers as injectable drug-delivery systems. *Nature*, 388 (6645), 860-862.
- [4] Kresge, C.T., Leonowicz, M.E., Roth, W.J., Vartuli, J.C. and Beck, J.S., 1992, Ordered mesoporous molecular sieves synthesized by a liquid-crystal template mechanism. *Nature*, 359 (6397), 710.
- [5] Wang, S., 2009, Ordered mesoporous materials for drug delivery, *Microporous and mesoporous materials*, 117 (1), 1-9.
- [6] Parveen, S. and Sahoo, S.K., 2008, Polymeric nanoparticles for cancer therapy. *Journal of drug targeting*, 16 (2), 108-123.
- [7] Sahoo, S.K., Parveen, S. and Panda, J.J., 2007, The present and future of nanotechnology in human health care, *Nanomedicine: Nanotechnology, Biology and Medicine*, 3 (1), 20-31.
- [8] Parveen, S., Misra, R. and Sahoo, S. K., 2012, Nanoparticles: a boon to drug delivery, therapeutics, diagnostics and imaging, *Nanomedicine: Nanotechnology, Biology and Medicine*, 8 (2), 147-166.
- [9] He, Q. and Shi, J., 2011, Mesoporous silica nanoparticle based on drug delivery systems: synthesis, controlled drug release and delivery, pharmacokinetics and biocompatibility, *Journal of Materials Chemistry*, 21 (16), 5845-5855.
- [10] Woodruff, C.W. and Nuessle, N.O., 1972, Effect of processing variables on particles obtained by extrusion—spheronization processing, *Journal of pharmaceutical sciences*, 61 (5), 787-790.
- [11] Marzouq, D.M.T. and Hodali, H.A.A., 2012, Use of mesoporous siliceous materials as drug delivery systems, master degree thesis, Jordanian university.
- [12] Al Mamori, F.F., Drawazeh, N. and Al Khatib, H., 2011, Effect of drug delivery system configuration on performance of multi-layered pellets, master degree thesis, Jordanian university.

- [13] Al Kasasbe, R.M., Khdair A., Abu Dahab, R., 2014, Evaluation of safety and uptake mechanism of a micellar drug delivery system based on poly ethyleneoxide) -B-poly (prpyleneoxide) (peo B- Pro) copolymers using caco-2 cell culture model, master degree thesis, Jordanian university.
- [14] Banker, R.D. and Morey, R.C., 1986, Efficiency analysis for exogenously fixed inputs and outputs, *Operations research*, 34 (4), 513-521.
- [15] Rane, M., Parmar, J. and Siahboomi, A.R., 2010, Hydrophilic matrices for oral extended release: influence of fillers on drug release from HPMC matrices. *Pharma Times*, 42 (4), 41-5.
- [16] Langer, R., 2000, Biomaterials in drug delivery and tissue engineering: one laboratory's experience, *Accounts of Chemical Research*, 33 (2), 94-101.
- [17] Bhadra, D., Bhadra, S., Jain, P. and Jain, N.K., 2002, Pegnology: a review of PEG-ylated systems. *Die Pharmazie*, 57 (1), 5-29.
- [18] Kommareddy, S., Tiwari, S.B. and Amiji, M.M., 2005, Long-circulating polymeric nanovectors for tumor-selective gene delivery, *Technology in cancer research & treatment*, 4 (6), 615-625. ISO 690.
- [19] Lee, M. and Kim, S.W., 2005, Polyethylene glycol-conjugated copolymers for plasmid DNA delivery, *Pharmaceutical research*, 22 (1), 1-10.
- [20] Mu, L. and Feng, S.S., 2003, A novel controlled release formulation for the anticancer drug paclitaxel (Taxol®): PLGA nanoparticles containing vitamin E TPGS. *Journal of controlled release*, 86 (1), 33-48.
- [21] Vila, A., Sanchez, A., Tobio, M., Calvo, P. and Alonso, M.J., 2002, Design of biodegradable particles for protein delivery, *Journal of Controlled Release*, 78 (1-3), 15-24.
- [22] Mohanraj, V.J. and Chen, Y., 2006, Nanoparticles-a review. *Tropical journal of pharmaceutical research*, 5 (1), 561-573.
- [23] Hett, A., 2004, *Nanotechnology: Small matter, many unknowns*. Swiss Reinsurance Company.
- [24] Xia, Y., Yang, P., Sun, Y., Wu, Y., Mayers, B., Gates, B. ... and Yan, H., 2003, One-dimensional nanostructures: synthesis, characterization, and applications. *Advanced materials*, 15 (5), 353-389.

- [25]Bhatia, S., 2016, Nanoparticles types, classification, characterization, fabrication methods and drug delivery applications, *In Natural Polymer Drug Delivery Systems*, pp. 33-93, Springer, Cham.
- [26]Tiwari, J. N., Tiwari, R. N. and Kim, K. S., 2012, Progress in Materials Science three-dimensional nanostructured materials for advanced electrochemical energy devices, *Progress in Materials Science*, 57 (4), 724–803, <https://doi.org/10.1016/j.pmatsci.2011.08.003>.
- [27]Khan, I., Saeed, K. and Khan, I., 2017, Nanoparticles: Properties, applications and toxicities, *Arabian Journal of Chemistry*.
- [28]Tourintio, F.A., Depeyrot, J., Da-Silva, G.J. and Lara, M.C.L., 1998, Analysis of FTIR spectra of nanoparticles, *Journal of Physics*, 28, 65-66.
- [29]Khan, I., Ali, S., Mansha, M. and Qurashi, A., 2017, Sonochemical assisted hydrothermal synthesis of pseudo-flower shaped Bismuth vanadate (BiVO₄) and their solar-driven water splitting application. *Ultrasonics sonochemistry*, 36, 386-392.
- [30]Khan, I., Ibrahim, A.A., Sohail, M., and Qurashi, A. 2017, Sonochemical assisted synthesis of RGO/ZnO nanowire arrays for photoelectrochemical water splitting, *Ultrasonics sonochemistry*, 37, 669-675.
- [31]Emery, A.A., Saal, J.E., Kirklin, S., Hegde, V.I. and Wolverton, C., 2016, High-throughput computational screening of perovskites for thermochemical water splitting applications, *Chemistry of Materials*, 28 (16), 5621-5634.
- [32]Herron, N. and Thorn, D.L., 1998, Nanoparticles: uses and relationships to molecular cluster compounds, *Advanced Materials*, 10 (15), 1173-1184.
- [33]Kuschel, A. and Polarz, S., 2008, Organosilica materials with bridging phenyl derivatives incorporated into the surfaces of mesoporous solids, *Advanced Functional Materials*, 18 (8), 1272-1280.
- [34]Mitra, A., Vázquez-Vázquez, C., López-Quintela, M.A., Paul, B.K. and Bhaumik, A., 2010, Soft-templating approach for the synthesis of high surface area and superparamagnetic mesoporous iron oxide materials. *Microporous and Mesoporous Materials*, 131 (1-3), 373-377.
- [35]Park, J.W., Jung, D.S., Seo, M.E., Kim, S.Y., Moon, W.J., Shin, C.H. and Seo, G., 2008, Preparation of mesoporous materials with adjustable pore size using anionic

- and cationic surfactants, *Microporous and Mesoporous Materials*, 112 (1-3), 458-466.
- [36]Pang, J.B., Qiu, K.Y. and Wee, Y., 2000, Synthesis of mesoporous silica materials with ascorbic acid as template via sol-gel process, *Chinese Journal of Chemistry*, 18 (5), 693-697.
- [37]Ryoo, R., 2009, Porous materials: A tricontinuous mesoporous system, *Nature chemistry*, 1 (2), 105.
- [38]Solano-Umaña, V. and Vega-Baudrit, J.R., 2015, Micro, Meso and Macro Porous Materials on Medicine, *Journal of Biomaterials and Nanobiotechnology*, 6 (4), 247.
- [39]Rouquerol, J., Avnir, D., Fairbridge, C.W., Everett, D.H., Haynes, J.M., Pernicone, N. and Unger, K.K., 1994, Recommendations for the characterization of porous solids, Technical Report, Pure and Applied Chemistry, 66 (8), 1739-1758.
- [40]Iravani, S., 2011, Green synthesis of metal nanoparticles using plants. *Green Chemistry*, 13 (10), 2638-2650.
- [41]Mogilevsky, G., Hartman, O., Emmons, E.D., Balboa, A., DeCoste, J.B., Schindler, B. J., ... and Karwacki, C.J., 2014, Bottom-up synthesis of anatase nanoparticles with graphene domains, *ACS applied materials & interfaces*, 6 (13), 10638-10648.
- [42]Liu, D., Li, C., Zhou, F., Zhang, T., Zhang, H., Li, X. ... and Li, Y., 2015, Rapid synthesis of monodisperse Au nanospheres through a laser irradiation-induced shape conversion, self-assembly and their electromagnetic coupling SERS enhancement, *Scientific reports*, 5, 76-86.
- [43]Liu, J., Liu, Y., Liu, N., Han, Y., Zhang, X., Huang, H. and Kang, Z., 2015, Metal-free efficient photocatalyst for stable visible water splitting via a two-electron pathway, *Science*, 347(6225), 970-974.
- [44]Wang, Y. and Xia, Y., 2004, Bottom-up and top-down approaches to the synthesis of monodispersed spherical colloids of low melting-point metals, *Nano Letters*, 4 (10), 2047-2050.
- [45]Bello, S.A., Agunsoye, J.O. and Hassan, S.B., 2015, Synthesis of coconut shell nanoparticles via a top down approach: Assessment of milling duration on the particle sizes and morphologies of coconut shell nanoparticles, *Materials Letters*, 159, 514-519.

- [46]Piao, Y., Burns, A., Kim, J., Wiesner, U. and Hyeon, T., 2008, Designed fabrication of silica-based nanostructured particle systems for nanomedicine applications. *Advanced Functional Materials*, 18 (23), 3745-3758.
- [47]Descalzo, A.B., Martínez-Máñez, R., Sancenon, F., Hoffmann, K. and Rurack, K., 2006, *The supramolecular chemistry of organic–inorganic hybrid materials*, Angewandte Chemie International Edition, 45 (36), 5924-5948. Chicago.
- [48]Trewyn, B.G., Slowing, I.I., Giri, S., Chen, H.T. and Lin, V.S.Y., 2007, Synthesis and functionalization of a mesoporous silica nanoparticle based on the sol–gel process and applications in controlled release. *Accounts of chemical research*, 40 (9), 846-853.
- [49]Vivero-Escoto, J.L., Slowing, I.I., Trewyn, B.G., & Lin, V.S.Y, 2010, Mesoporous silica nanoparticles for intracellular controlled drug delivery, *Small*, 6 (18), 1952-1967.
- [50]Lee, B.K., Yun, Y.H. and Park, K., 2015, Smart nanoparticles for drug delivery: Boundaries and opportunities, *Chemical engineering science*, 125, 158-164.
- [51]Smolen, V.F., and Ball, L., 1984, Controlled drug bioavailability: volume 2, bioavailability methodology and regulation.
- [52]Cleary, G.W., Lange, R.S. and Wise, D.L., 1984, Medical applications of controlled release, *Transdermal controlled release systems, Boca Raton FL: CRC*, 203-51.
- [53]Banakar, U.V., 1987, Drug delivery systems of the 90s: Innovations in controlled release, *American pharmacy*, 27 (2), 39-44.
- [54]Robinson, J. and Lee, V.H., 1987, Controlled drug delivery: fundamentals and applications. CRC Press.
- [55]Vallet-Regi, M., Ramila, A., Del Real, R.P. and Pérez-Pariente, J., 2001, A new property of MCM-41: drug delivery system, *Chemistry of Materials*, 13 (2), 308-311.
- [56]Zhao, D., Feng, J., Huo, Q., Melosh, N., Fredrickson, G.H., Chmelka, B.F. and Stucky, G.D., 1998, Triblock copolymer syntheses of mesoporous silica with periodic 50 to 300 angstrom pores, *Science*, 279 (5350), 548-552.
- [57]Meng, Y., GU, D., Zhang, F., Shi, Y., Yang, H., Li, Z. ... and Zhao, D., 2005, Ordered mesoporous polymers and homologous carbon frameworks: amphiphilic

- surfactant templating and direct transformation, *Angewandte Chemie*, 117 (43), 7215-7221.
- [58] Fournier, E., Passirani, C., Montero-Menei, C.N. and Benoit, J.P., 2003, Biocompatibility of implantable synthetic polymeric drug carriers: focus on brain biocompatibility. *Biomaterials*, 24 (19), 3311-3331.
- [59] Lin, V.S.Y., Lai, C.Y., Huang, J., Song, S.A. and Xu, S., 2001, Molecular recognition inside of multifunctionalized mesoporous silicas: toward selective fluorescence detection of dopamine and glucosamine. *Journal of the American Chemical Society*, 123 (46), 11510-11511.
- [60] Mal, N.K., Fujiwara, M. and Tanaka, Y., 2003, Photo controlled reversible release of guest molecules from coumarin-modified mesoporous silica, *Nature*, 421 (6921), 350.
- [61] Tourné-Péteilh, C., Brunel, D., Bégu, S., Chiche, B., Fajula, F., Lerner, D.A. and Devoisselle, J.M., 2003, Synthesis and characterisation of ibuprofen-anchored MCM-41 silica and silica gel. *New Journal of Chemistry*, 27 (10), 1415-1418.
- [62] Singhvi, G. and Singh, M., 2011, In-vitro drug release characterization models, *International Journal of Pharmaceutical Studies and Research*, 2, 77-84.
- [63] Higuchi, W.I., 1967, Diffusional models useful in biopharmaceutics, Drug release rate processes, *Journal of pharmaceutical sciences*, 56 (3), 315-324.
- [64] Noyes, A.A. and Whitney, W.R., 1897, The rate of solution of solid substances in their own solutions, *Journal of the American Chemical Society*, 19 (12), 930-934.
- [65] Lakshmi, P.K., 2010, Dissolution testing is widely used in the pharmaceutical industry for optimization of formulation and quality control of different dosage forms, *Pharma info. net*.
- [66] Gohel, M.C., Panchal, M.K. and Jogani, V.V., 2000, Novel mathematical method for quantitative expression of deviation from the Higuchi model. *AAPS PharmSciTech*, 1(4), 43-48.
- [67] Davis, S.S., Illum, L. and Stolnik, S., 1996, Polymers in drug delivery, *Current Opinion in Colloid & Interface Science*, 1 (5), 660-666.
- [68] Korsmeyer, R.W., Gurny, R., Doelker, E., Buri, P. and Peppas, N.A., 1983, Mechanisms of solute release from porous hydrophilic polymers, *International journal of pharmaceuticals*, 15 (1), 25-35.

- [69]Zhou, H., Sun, J., Wu, X., Ren, B. and Wang, J.,2013, Tailored morphology and controlled structure of bimodal mesopores silicas via additive ammonia amount in the TEOS–CTAB–H₂O system, *Materials Chemistry and Physics*, 140 (1), 148-153.
- [70]Ganesh, M. and Lee, S.G., 2013, Synthesis, characterization and drug release capability of new cost effective mesoporous silica nano particle for ibuprofen drug delivery, *Int J Cont Auto*, 6, 207-16.
- [71]Illangakoon, U.E., Nazir, T., Williams, G.R. and Chatterton, N.P., 2014, Mebeverine-Loaded Electrospun Nanofibers: Physicochemical Characterization and Dissolution Studies, *Journal of pharmaceutical sciences*, 103 (1), 283-292.
- [72]Anal, A.K., Bhowmik, D., Gopinath, H., Kumar, B.P., Duraivel, S., Kumar, K.P.S.... and Mohamadnia, F., 2010, Modeling and comparison of dissolution profiles, *Medical Hypotheses*, 13 (3), 123-133. [https://doi.org/10.1016/S0928-0987\(01\)00095-1](https://doi.org/10.1016/S0928-0987(01)00095-1).
- [73]Olukman, M., Peng, Z., She, M. F. and Hong, L. 2010, Physiochemical property and morphology of 5-fluorouracil loaded chitosan nanoparticles, *International conference on nanoscience and nanotechnology*, (ICONN), Sydney, Australia 248-250.
- [74]Adlnasab, L., Shabaniyan, M., Ezoddin, M. and Maghsodi, A., 2017, Amine rich functionalized mesoporous silica for the effective removal of alizarin yellow and phenol red dyes from waste waters based on response surface methodology, *Materials Science & Engineering B*, 226 (June), 188–198.
- [75]Cauda, V., Argyo, C., Schlossbauer, A. and Bein, Th., 2010, Controlling the delivery kinetics from colloidal mesoporous silica nanoparticles with pH-sensitive gates, *Journal of Materials Chemistry*, 4305–4311.
- [76]Aw, M. S., Simovic, S., Yu, Y., Addai-Mensah, J. and Losic, D., 2012, Porous silica microshells from diatoms as biocarrier for drug delivery applications, *Powder Technology*, 223 (2012) 52–58.

CURRICULUM VITAE

Personal Information	
Name Surname	MONA H. ALI BNHMAD
Place of Birth	Elmarj, Libya
Date of Birth	23.06 1988
Nationality	<input type="checkbox"/> T.C. <input checked="" type="checkbox"/> Other: LIBYAN
Phone Number	05417699561
Email	moonlibya002@gmail.com
Web Page	



Educational Information	
B. Sc.	
University	University Of Benghazi
Faculty	Science
Department	Chemistry
Graduation Year	2011-2012

M. Sc.	
University	Istanbul University-Cerrahpasa
Institute	Institute of graduate studies in science and engineering
Department	Department of Chemistry
Programme	Chemistry

Publications	
1. Aroğuz A.Z., Alibenhmid, M., Rahimpour J., "Drug Release Capability of Mesoporous Nano-Silica (MNS) for Acetyl cysteine ", Uluslararası VII. Polimer Bilim ve Teknoloji kongresi, ESKİŞEHİR, TÜRKİYE, 9-12 Eylül 2018, pp.415-415.	
2. Rahimpour J., Alibenhmid, M., Aroğuz A.Z., "Preparation of Mesoporous Nano-Silica (MNS) as Adsorbent", 5th Iran International Zeolite Conference, Tebriz, IRAN, 26-27 Ağustos 2018, pp.281-284.	